DLMP-based Quantification and Analysis Method of Operational Flexibility in Flexible Distribution Networks

Jie Jian, *Student Member*, *IEEE*, Peng Li, *Senior Member*, *IEEE*, Haoran Ji*, *Member*, *IEEE*, Linquan Bai, *Senior Member*, *IEEE*, Hao Yu, *Member*, *IEEE*, Wei Xi, Jianzhong Wu, *Member*, *IEEE*, Chengshan Wang, *Senior Member*, *IEEE*

***Abstract*—With high penetration of flexible resources, operational flexibility of flexible distribution networks (FDNs) is important to ensure high-quality electricity services. This paper proposes a value quantification and analysis method for operational flexibility in FDNs based on distribution locational marginal pricing (DLMP). First, flexibility constraints are formulated from the perspective of node integration, branch transfer, and network aggregation of flexibility. Then, a unified analytical framework for quantifying the operational flexibility is established, in which spatial-temporal transfer of flexibility is modeled with the derivation of flexibility sensitivity factors. Further, a DLMP-based flexibility value quantification model is proposed with nodal net power as the unit for flexibility pricing. The obtained flexibility price can not only quantify flexibility value but also be used to guide the flexible resources. Finally, the effectiveness of the proposed method is validated on a modified IEEE 33-node distribution system and a modified IEEE 123-node distribution system. Results verify that the proposed method can quantify the impact of nodal net power on operational flexibility and effectively improve the overall flexibility performance through the guide of flexibility price.**

***Index Terms*—flexible distribution network (FDN), distributed generator (DG), operational flexibility, quantification, distribution locational marginal pricing (DLMP).**

NOMENCLATURE

Abbreviation

DER	Distributed energy resource
DG	Distributed generator
FDN	Flexible distribution network
DSO	Distribution system operator
DLMP	Distribution locational marginal pricing
SOP	Soft open point
ESS	Energy storage system
DL	Delay-tolerant load
PV	Photovoltaic
WT	Wind turbine
TL	Time-sensitive load

Sets

Ω_{n}	Set of all nodes
Ω_{b}	Set of all branches
Ω_{res}	Set of flexible resources which can provide reserve
$\Omega(i)$	Set of branches connected to node i
$\xi(i)$	Set of branches between node i and source node
Ω_{T}	Set of time slots
$\Omega_{\mathrm{DG}}, \Omega_{\mathrm{DL}}, \Omega_{\mathrm{SOP}}, \Omega_{\mathrm{ESS}}$	Sets of DGs, DLs, SOPs, and ESSs
$\Omega_{\mathrm{FR}}^{\mathrm{P}}, \Omega_{\mathrm{FR}}^{\mathrm{Q}}$	Set of flexible resources which can provide active/ reactive power services

Indices

i, k	Indices of nodes
t	Indices of time slots

Variables

$V_{i,t}$	Voltage magnitude at node i in time t
$P_t^{\mathrm{sub}}, Q_t^{\mathrm{sub}}$	Aggregated active/reactive power interacted with upper grid in time t
$P_t^{\mathrm{loss}}, Q_t^{\mathrm{loss}}$	Active/reactive power losses of network at node i in time t
$P_{i,t}^{\mathrm{bus}}, Q_{i,t}^{\mathrm{bus}}$	Nodal net active/reactive power at node i in time t
$P_{l,t}, Q_{l,t}$	Active/reactive power flow of branch l in time t
$P_{i,t}^{\mathrm{SOP}}, Q_{i,t}^{\mathrm{SOP}}$	Active/reactive power output of SOP at node i in time t
$P_{i,t}^{\mathrm{ESS}}, Q_{i,t}^{\mathrm{ESS}}$	Active/reactive power output of ESS at node i in time t
$P_{i,t}^{\mathrm{SOP,L}}, P_{i,t}^{\mathrm{ESS,L}}$	Active power losses of SOP and ESS converters at node i, respectively
$P_{i.t}^{\mathrm{DG}}, Q_{i,t}^{\mathrm{DG}}$	Active/reactive power injection by DG at node i at time t (kW, kvar)
$P_{i,t}^{\mathrm{TL}}, Q_{i,t}^{\mathrm{TL}}$	Active/reactive power consumption of TL at node i in time t

This work was supported by the National Key R&D Program of China (2020YFB0906000, 2020YFB0906002).

P. Li, J. Jian, H. Ji, H. Yu, and C. Wang are with the Key Laboratory of Smart Grid of Ministry of Education, Tianjin University, Tianjin 300072, China (email: jihaoran@tju.edu.cn).

Wei Xi is with the Digital Grid Research Institute, China Southern Power Grid, Guangzhou 510670, China, and also with the Key Laboratory of Smart Grid of Ministry of Education, Tianjin University, Tianjin 300072, China (e-mail: xiwei@csg.cn).

L. Bai is with the Department of Systems Engineering and Engineering Management, University of North Carolina at Charlotte, Charlotte, NC 28223 USA (email: linquanbai@uncc.edu).

J. Wu is with the Institute of Energy, School of Engineering, Cardiff University, Cardiff CF24 3AA, U.K. (email: wuj5@cardiff.ac.uk).

$P_{i,t}^{\mathrm{DL}}, Q_{i,t}^{\mathrm{DL}}$ Active/reactive power consumption of DL at node i in time t

$P_{i,t}^{\mathrm{FR}}, Q_{i,t}^{\mathrm{FR}}$ Active/reactive power of flexible resources at node i in time t

$R_{i,t}^{\mathrm{up}}, R_{i,t}^{\mathrm{down}}$ Upward/downward reserve of flexible resource providing power reserve at node i in time t

$E_{i,t}^{\mathrm{ESS}}$ SOC of ESS at node i in time t

$E_{i,t}^{\mathrm{DL}}$ Energy stored of DL at node i in time t

$\varphi_{i,t}$ Flexibility payment or revenue of nodal net power at node i in time t

$\pi_{i,t}^{\mathrm{P}}, \pi_{i,t}^{\mathrm{Q}}$ Flexibility price of unit active/reactive power at node i in time t

$\pi_{i,t}^{\mathrm{P,Bus}}$, $\pi_{i,t}^{\mathrm{Q,Bus}}$, Node flexibility price of unit active/reactive power at node i in time t

$\pi_{i,t}^{\mathrm{P,Bran}}$, $\pi_{i,t}^{\mathrm{Q,Bran}}$ Branch flexibility price of unit active/reactive power at node i in time t

$\pi_{i,t}^{\mathrm{P,Net}}$, $\pi_{i,t}^{\mathrm{Q,Net}}$ Network flexibility price of unit active/reactive power at node i in time t

$\lambda_i^{\mathrm{Pbus}}, \lambda_i^{\mathrm{Qbus}}$ Lagrange multipliers of nodal net power constraints

$\mu_i^{\mathrm{v},-}, \mu_i^{\mathrm{v},+}$ Lagrange multipliers of nodal voltage flexibility constraints

$\mu_{l,c}$ Lagrange multiplier of branch transfer flexibility constraints

$\lambda^{\mathrm{P}}, \lambda^{\mathrm{Q}}$ Lagrange multipliers of network aggregation flexibility constraints

$\mu_i^{\mathrm{R1}}, \mu_i^{\mathrm{R2}}$ Lagrange multipliers of network flexibility reserve constraints

Parameters

$N_{\mathrm{N}}, N_{\mathrm{b}}, N_{\mathrm{T}}$ Total number of nodes, branches, and time slots

$V_{\min}, V_{\max}$ Upper/lower limits of nodal voltage

$\underline{V}_{\mathrm{flx}}, \bar{V}_{\mathrm{flx}}$ Upper/lower limits of desired nodal voltage

r_l, x_l Resistance/reactance of branch l

$S_{l,\max}$ Capacity limit of branch l

$F_{i,t}^{\mathrm{P}}, F_{i,t}^{\mathrm{Q}}$ Active/reactive nodal loss terms at node i in time t

$P_{i,t}^{\mathrm{DG,ref}}$ Forecasted active power generated by DG at node i in time t

$S_i^{\mathrm{DG}}, S_i^{\mathrm{SOP}}$ Capacity limits of DG/SOP at node i

$\bar{P}_i^{\mathrm{SOP}}, \underline{P}_i^{\mathrm{SOP}}$ Upper/lower limits of active power output of SOP at node i

$\bar{Q}_i^{\mathrm{SOP}}, \underline{Q}_i^{\mathrm{SOP}}$ Upper/lower limits of reactive power output of SOP at node i

$\bar{P}_i^{\mathrm{ESS}}, \underline{P}_i^{\mathrm{ESS}}$ Upper/lower limits of active power output of ESS at node i

$\bar{Q}_i^{\mathrm{ESS}}, \underline{Q}_i^{\mathrm{ESS}}$ Upper/lower limits of reactive power output of ESS at node i

$\bar{P}_i^{\mathrm{DL}}$ Upper limits of active power consumption of DL at node i

$\bar{E}_i^{\mathrm{ESS}}, \underline{E}_i^{\mathrm{ESS}}$ Upper/lower limits of SOC of ESS at node i

$\bar{E}_i^{\mathrm{DL}}, \underline{E}_i^{\mathrm{DL}}$ Upper/lower limits of SOC of DL at node i

$E_i^{\mathrm{DL,req}}$ Required SOC of DL at node i

$A_i^{\mathrm{E,L}}, A_i^{\mathrm{S,L}}$ Loss coefficients of ESS/SOP converter at node i

Δt dispatch horizon

β Reserve ratio

$\alpha_{c,0}, \alpha_{c,1}, \alpha_{c,2}$ Constant coefficients of approximate polygon expressions

$P_{i,t}^{\mathrm{TL,ref}}$, $Q_{i,t}^{\mathrm{TL,ref}}$ Scheduled active/reactive power consumption of TL at node i in time t

$T_{i,\mathrm{st}}^{\mathrm{DL}}$ The start charging time of DL at node i

$T_{i,\mathrm{req}}^{\mathrm{DL}}$ The desired time that SOC of DL meets the requirements at node i

M_{l-i} Branch-node incidence element between branch l and node i in time t

$D_i^{\mathrm{VP}}, D_i^{\mathrm{VQ}}$ Nodal flexibility sensitivity factors of nodal net active/reactive power at node i to nodal voltage in time t

$B_{l-i}^{\mathrm{PP}}, B_{l-i}^{\mathrm{QQ}}, B_{l-i}^{\mathrm{PQ}}, B_{l-i}^{\mathrm{QP}}$ Branch flexibility sensitivity factors of nodal net active/reactive power at node i to active/reactive power transfer on branch l in time t

L_i^{PP}, L_i^{PQ}, L_i^{QP}, L_i^{QQ} Network flexibility sensitivity factors of nodal net active/reactive power at node i to network loss in time t

I. Introduction

The integration of high-penetration of DERs such as DGs and flexible loads becomes a trend in distribution networks for the usage of renewable energy and customized electricity service [1]. However, resources with multiple operational characteristics and requirements will greatly increase the complexity of system operation management [2]. Distribution networks undergo drastically uneven spatial and temporal distribution of power generation and demand [3]. Without proper power dispatch, it may result in serious operational issues, such as heavy branch congestion, voltage violations, and unnecessary network losses [4].

Accordingly, distribution networks are evolving towards FDN to adapt to complex environments [5]. As for physical foundations, the wide use of advanced power electronics on the source, network, and demand sides enables FDNs with enhanced controllability and flexibility [6]. As for theoretical methodologies, operational flexibility analysis is crucial for FDNs to properly dispatch flexible resources and thus flexibly accommodate the high penetration of DERs [7]. It is indispensable to evaluate operational flexibility and exploit flexibility potential to maximize operational profits of FDNs [8].

Operational flexibility of distribution networks has been widely investigated in existing works [9]. At present, the generally recognized definitions of operational flexibility were proposed by the North American Electric Reliability Corporation (NERC) and the International Energy Agency (IEA). According to NERC, operational flexibility is defined as the ability to satisfy the variation of loads by using available resources in a system [10]. According to IEA, operational flexibility is defined as the ability to rapidly respond to predictable and unpredictable power fluctuations and guarantee the balance of generation and demand [11]. Similar to the above definitions, Mark O' Malley *et al* regarded flexibility as the

ability to respond to load variations [12]. Lu *et al.* defined it as the system's ability to adapt to source-network-demand sides' random variation by optimizing available resources within a certain cost under given timescales [13]. As stated in existing research, the focus of operational flexibility is to mitigate power fluctuations and guarantee a secure and high-performance system operating with high DER penetration. Research on operational flexibility of distribution networks can be classified into two main categories as follows:

1) Quantification methods of operational flexibility. Some novel quantification approaches have been proposed, which effectively evaluated the flexibility performance or visualized the flexibility regions of distribution networks. Ref. [14] proposed an interesting flexibility metric to evaluate the excessive availability of a system. It was further used to visualize the flexibility region of net loads. Ref. [15] designed a novel flexibility assessment method to quantify the renewable output in various regions for tackling renewable power fluctuations. Ref. [16] invented an innovative quantification method and obtained an approximate feasible region of net power injection.

These flexibility quantification methods have explored the allowable region of power considering various flexibility factors [17]. However, the large amounts of flexible resources at the source, network, and demand sides are with various operation characteristics. Flexibility quantification becomes a complex highly-dimensional projection problem [18]. In addition, the geographically dispersed flexible resources may impact the availability and requirements of operational flexibility at different locations. It may remain unrevealed that spatial-temporal transfer relationships of operational flexibility in distribution networks. Thus, a generalized comprehensive analytic framework is necessary to quantify operational flexibility of FDNs with multiple flexible resources.

2) Improvement methods of operational flexibility. The optimal dispatch strategy can improve system operation performance with enhanced accommodation of DERs [19]. Ref. [20] proposed a novel flexibility improvement method for DSO, which was applicable regardless of the topology of network. In Ref. [21], a risk-averse strategy was determined considering the coordination of DGs, SOPs, and demand response for flexible improvement. Ref. [22] presented an extensive analysis of multiple flexibility options to cope with the intermittence of DG generation, in which demand response, ESSs, and network reconfiguration were considered.

However, it is increasingly complex to determine a feasible solution that can satisfy diversified flexibility requirements without violating various operational constraints. Also in many approaches, DSO will send dispatch schedules to devices but may not be able to interpret the flexibility value of power demand or supply at different nodes to distribution networks. Thus, flexible resources in distribution networks may lack sufficient incentives to follow the dispatch. It is worth mentioning that the same amount of flexibility service at various locations in different time slots may have opposing flexibility values. Hence, it still needs a further investigation on how to formulate operational flexibility constraints and requires an explicit analytic solution to motivate resources to provide flexibility.

In distribution networks, nodal net power reflects the integration of various resources at a node. Various adjustment capabilities of flexible resources and differentiated flexible services can be standardized, thereby significantly reducing the difficulty of flexibility analysis and dispatch. Net power of all nodes will be transmitted through branches and finally be aggregated to interact with the external grid. Nodal net active and reactive power can be regarded as the basic adjustment units of operational flexibility in FDNs.

To fill the above research gaps on operational flexibility, a generalized analytic framework based on nodal net power is proposed for flexibility analysis and flexibility dispatch in FDNs. First, from the perspective of operational flexibility, operational states and related constraints of distribution networks can be reinterpreted and classified into node integration, branch transfer, and network aggregation flexibility. Based on the above comprehensive analysis foundation, the mathematical analytic model of spatial-temporal transfer of operational flexibility is proposed. Flexibility sensitivity factors are derived to analytically represent the spatial-temporal transfer relationship of operational flexibility.

Further, to apply the above flexibility transfer analysis in flexibility dispatch, pricing the power flexibility at the distribution network level is regarded as a promising approach [23]. Currently, power controllability and flexibility of resources have promoted the emergence of prosumers in FDNs. Prosumers can both purchase electricity based on demands and sell services according to system operational status [24]. Proper flexibility pricing methodology can price the flexibility value and be used to guide the dispatch of flexible resources [25].

To quantify the flexibility value in a generalized pricing framework, DLMP [26] can be adopted. DLMPs are derived based on dual variables of the primal model at its optimum [27]. According to duality analysis, DLMP reflects the incremental marginal total cost for adding one more unit of nodal net power in a time slot under an operation strategy in distribution networks [28]. It has been widely studied in some meaningful works for congestion management [29], demand-side response [30], DG impact analysis [31], and calculation accuracy of DLMP [32]. Based on this analysis, DLMP has also been used to price electricity products in trading mechanism design [33]. The above works have verified the incentive application of DLMP on system operation management.

Thus, it is promising to price power flexibility based on DLMP at the distribution network level. It can quantify the unit flexibility value of nodal net power in the form of price, which is similar to the concept of the currency exchange rate in the financial industry. It could be an effective price incentive [34] for DSO to guide and coordinate the system-wide flexible resources to achieve a feasible balance of diversified flexibility requirements in FDNs. However, research on DLMP derivation of distribution networks generally uses the DCOPF model or the linearized ACOPF model by ignoring the reactive power component or the power loss term. It can improve

computational efficiency but may cause the deviation of calculation results from the real values [35].

To reconcile computation efficiency with modeling accuracy of DLMP, the modified linearized Distflow model is adopted with the nodal loss model [36] to consider the power losses in branch transfer flexibility analysis. Further, a DLMP-based flexibility pricing methodology is proposed, which is compatible with the explicit analytic expressions of spatial-temporal transfer relationships of operational flexibility. The flexibility price is determined by deducing DLMP of the linearized flexibility constraints of FDNs [37]. It provides users insight into the flexibility value of their power adjustments.

Thus, the operational problems of distribution networks are interpreted from the perspective of operational flexibility, including node integration, branch transfer, and network aggregation flexibility. Based on the analytic framework, a DLMP-based flexibility pricing method is proposed to quantify the flexibility value and determine the amount of nodal net power. Then, the DLMP-based flexibility price is utilized as an incentive signal for flexible resource dispatch to improve the operational benefits of FDNs. The main contributions are summarized as follows:

1) First, flexibility constraints are formulated for a comprehensive analysis of operational flexibility, including node integration, branch transfer, and network aggregation flexibility of FDNs. Flexibility sensitivity factors are derived to analytically represent the spatial-temporal transfer relationship of operational flexibility. An analytic framework of operational flexibility is proposed based on nodal net power to achieve a feasible balance of diversified flexibility requirements.

2) Then, a DLMP-based flexibility quantification model is proposed for FDNs with multiple flexible resources. The DLMP-based flexibility pricing not only quantifies the flexibility value of nodal net power on operational flexibility in the form of price but also is used for the spatial-temporal balance of operational flexibility. As the price reflects power dispatch at each node for the same worth of flexibility service, it can be used to guide flexible resources to improve diversified flexibility performance.

The remainder of this paper is organized as follows. Section II describes the developed flexibility constraints and proposes the mathematical analytic model of operational flexibility, in which flexibility sensitivity factors are derived. Section III further proposes the DLMP-based flexibility pricing model based on the linearized transfer relationship of operational flexibility. In Section IV, the DLMP-based flexibility price is obtained for quantification of spatial-temporal flexibility, which can be used to motivate flexible resources. The case studies on a modified IEEE 33-node test case and a modified IEEE 123-node test case are given in Section V. The conclusions and prospects are stated in Section VI.

II. Analytic Model of Operational Flexibility

In this section, operational flexibility of FDNs is described from the perspective of node integration, branch transfer, and network aggregation. Related flexibility constraints are developed and a linearized transfer model of operational flexibility in distribution networks is proposed. Flexibility sensitivity factors are calculated, which lay the foundation for flexibility quantification and strategy determination.

A. Formulation of Operational Flexibility Constraints

1) Node flexibility constraints

Node integration flexibility reflects the local flexibility demand and supply states based on the impact analysis of nodal net power on nodal voltage.

Generally, system operation is influenced by nodal power injection and export. Flexible resources can be coordinated at the node level. Thus, node integration flexibility acts as the basic property of operational flexibility. It is described using nodal net power and nodal voltage range.

(1) Nodal net power

Nodal net power lays the foundation of the generalized analytical framework of operational flexibility.

Assuming that the positive direction is to export power from distribution networks, nodal net power can be expressed in (1).

$$\begin{aligned} P_{i,t}^{\mathrm{bus}} &= P_{i,t}^{\mathrm{TL}} + P_{i,t}^{\mathrm{DL}} - P_{i,t}^{\mathrm{DG}} - P_{i,t}^{\mathrm{ESS}} - P_{i,t}^{\mathrm{SOP}} \ (\lambda_i^{\mathrm{Pbus}}) \\ Q_{i,t}^{\mathrm{bus}} &= Q_{i,t}^{\mathrm{TL}} + Q_{i,t}^{\mathrm{DL}} - Q_{i,t}^{\mathrm{DG}} - Q_{i,t}^{\mathrm{ESS}} - Q_{i,t}^{\mathrm{SOP}} \ (\lambda_i^{\mathrm{Qbus}}) \end{aligned} \tag{1}$$

(2) Nodal voltage range

Nodal voltage is a critical index to quantify nodal flexibility. The nodal voltage beyond allowable range (2.a) means that the node is extremely lacking voltage flexibility. Electrical devices at such a node will be forced to be out of the grid, resulting in economic loss. The node with enough nodal flexibility can provide support to improve nodal voltage to desired range (2.b).

$$V_{\min} \le V_{i,t} \le V_{\max} \tag{2.a}$$

$$\underline{V}_{\mathrm{flx}} \le V_{i,t} \le \overline{V}_{\mathrm{flx}} \tag{2.b}$$

2) Branch flexibility constraints

Affected by the spatial distribution of flexile resources in the FDN, node flexibility may vary at different locations. The branch is essential to provide feasible transfer flexibility to balance the power demand and supply at different nodes. Meanwhile, the spatial balance of node flexibility is at the expense of certain transfer flexibility.

Branch transfer flexibility reflects the ability to transfer local flexibility for the spatial-temporal balance of flexibility based on the impact analysis of power transfer in distribution networks In (3.a), branch capacity is used to describe transfer flexibility. Network loss is used to describe the transfer expense of dispersed node flexibility in the form of energy in (3.b).

$$P_{l,t}^2 + Q_{l,t}^2 \le S_l^2 \tag{3.a}$$

$$\begin{aligned} P_t^{\mathrm{loss}} &= \textstyle\sum_{l\in\Omega_{\mathrm{b}}} r_l (P_{l,t}^2 + Q_{l,t}^2) \,/ V_{i,t}^2 \\ Q_t^{\mathrm{loss}} &= \textstyle\sum_{l\in\Omega_{\mathrm{b}}} x_l (P_{l,t}^2 + Q_{l,t}^2) \,/ V_{i,t}^2 \end{aligned} \tag{3.b}$$

where $V_{i,t}$ is assumed to denote voltage amplitude of node i which is the downstream node of branch l in time t.

3) Network flexibility constraints

The system-wide flexible resources can be coordinated to satisfy spatial-temporal requirements of node flexibility within the FDN. It can reduce the dependence on flexibility support

from the external grid. Network aggregation flexibility reflects the power self-sufficiency degree of distribution networks as well as operating reserves to satisfy the variation of aggregated power within a certain range.

(1) Network aggregation flexibility

A system with enough network flexibility can conduct bidirectional interaction of aggregated flexibility with the external grid, as formulated in (4).

$$P_t^{\text{sub}} = \sum_{i\in\Omega_{\text{n}}} P_{i,t}^{\text{bus}} + P_t^{\text{loss}},\ Q_t^{\text{sub}} = \sum_{i\in\Omega_{\text{n}}} Q_{i,t}^{\text{bus}} + Q_t^{\text{loss}} \quad (4)$$

(2) Network flexibility reserve

The aggregated power interaction with the external grid is generally determined in the day-ahead timeframe. However, real-time fluctuations of DGs and flexible loads may lead to the deviation of aggregated power from the estimated value.

The advance in power electronics allows flexible resources to adjust active and reactive power outputs rapidly and continuously. Thus, to enhance the operational flexibility of FDNs, flexible resources can provide operating reserves to satisfy the variation of aggregated power within a certain range.

The available reserve of a flexible resource is related to its allowable operation range and pre-determined schedule. The general form of range constraints is as follows:

$$0 \le R_{i,t}^{\text{up}} \le P_{i,t,\max}^{\text{FR}} - P_{i,t}^{\text{FR}}, \quad i \in \Omega_{\text{res}} \quad (5.a)$$

$$0 \le R_{i,t}^{\text{down}} \le P_{i,t}^{\text{FR}} - P_{i,t,\min}^{\text{FR}}, \quad (5.b)$$

$$\sum_{i\in\Omega_{\text{res}}}(R_{i,t}^{\text{up}} + R_{i,t}^{\text{down}}) \ge \beta\left|\sum_{i\in\Omega_{\text{n}}} P_{i,t}^{\text{bus}}\right| \quad (5.c)$$

where $P_{i,t,\max}^{\text{FR}}$ and $P_{i,t,\min}^{\text{FR}}$ are maximum and minimum available power of flexible resources at node i in time t, respectively.

The network flexibility reserve includes upward and downward reserves in (5.a)-(5.b). Assume that the positive direction of flexible resources is to inject power into a distribution system. The upward reserve is the margin to inject power. Assume that network flexibility reserve should be able to cope with the power change within at least β ($0\le \beta \le 100\%$) of the absolute value of summed nodal net active power in (5.c).

Note that the formulation of flexibility constraints originates from the power flow constraints of distribution networks. This comprehensive analysis foundation aims to guarantee that the generalized analytic framework of operational flexibility is proposed without violating operational constraints of FDNs.

B. Linearized Transfer Model of Operational Flexibility

The aggregation of dispersed local flexibility is realized through the spatial-temporal transfer of nodal net power. The spatial-temporal transfer relationship of operational flexibility is formulated as an explicit analytic expression in the form of flexibility sensitivity factors.

The modified linearized Distflow model is adopted in (6.a)-(6.b). To improve computational accuracy, a nodal loss model [36] is added to present power losses as flexibility expense during branch transfer. Assume that the positive direction is from parent node $i-1$ to i.

$$\begin{aligned} &P_{l,t} = P_{l-1,t} - \left(P_{i,t}^{\text{bus}} + F_{i,t}^{\text{P}}\right), Q_{l,t} = Q_{l-1,t} - \left(Q_{i,t}^{\text{bus}} + F_{i,t}^{\text{Q}}\right) \\ &V_{i,t} = V_{i-1,t} - \left[r_l\left(P_{i,t}^{\text{bus}} + F_{i,t}^{\text{P}}\right) + x_l\left(Q_{i,t}^{\text{bus}} + F_{i,t}^{\text{Q}}\right)\right]/V_{0,t} \end{aligned} \quad (6.a)$$

$$F_{i,t}^{\text{P}} = \frac{\sum_{l\in\xi(i)} r_l(P_{l,t}^{*2} + Q_{l,t}^{*2})}{2},\ F_{i,t}^{\text{Q}} = \frac{\sum_{l\in\xi(i)} x_l(P_{l,t}^{*2} + Q_{l,t}^{*2})}{2} \quad (6.b)$$

where $V_{0,t}$ is voltage of the source node in time t, $V_{0,t} \equiv 1$ p.u.. (6.b) lists the nodal loss equation. The loss on a branch is evenly divided and then added to its two end nodes. To remain linear, the nodal loss is calculated using the historical or day-ahead dispatch information of power flows.

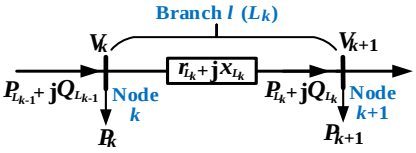

Fig. 1 Illustration of power flow of branch L_k.

For the sake of analysis, nodes and branches in the distribution network are numbered in Appendix A. Fig. 1 illustrates the transfer relationship between nodes and branches. The linearized model of flexibility transfer is formulated in (6.c)-(6.e).

$$\begin{aligned} P_{l,t} &= P_{L_k,t} = \sum_{i=k+1}^{N_{\text{n}}} M_{l-i}\left(P_{i,t}^{\text{bus}} + F_{i,t}^{\text{P}}\right) \\ Q_{l,t} &= Q_{L_k,t} = \sum_{i=k+1}^{N_{\text{n}}} M_{l-i}\left(Q_{i,t}^{\text{bus}} + F_{i,t}^{\text{Q}}\right) \end{aligned} \quad (6.c)$$

$$\begin{aligned} \Delta V_{i,t} &= V_{0,t} - V_{i,t} \approx \sum_{l\in\xi(i)}(r_l P_{l,t} + x_l Q_{l,t}) \\ &= \sum_{l\in\xi(i)}\sum_{i=k+1}^{N_{\text{n}}} M_{l-i}\left[r_l\left(P_{i,t}^{\text{bus}} + F_{i,t}^{\text{P}}\right) + x_l\left(Q_{i,t}^{\text{bus}} + F_{i,t}^{\text{Q}}\right)\right] \end{aligned} \quad (6.d)$$

$$\begin{aligned} P_t^{\text{loss}} &= \sum_{l\in\Omega_{\text{b}}} r_l\left(P_{l,t}^{*\,2} + Q_{l,t}^{*\,2}\right) \\ Q_t^{\text{loss}} &= \sum_{l\in\Omega_{\text{b}}} x_l\left(P_{l,t}^{*\,2} + Q_{l,t}^{*\,2}\right) \end{aligned} \quad (6.e)$$

For simplicity, sensitivity factors, branch-node incidence elements, and dual variables following omit the subscript t.

C. Calculation of Flexibility Sensitivity Factors

Flexibility sensitivity factors of nodal voltage, branch transfer, and network loss are calculated as follows.

1) Nodal voltage sensitivity

Nodal voltage sensitivity is obtained by calculating the derivative of the nodal net power for nodal voltage deviation (6.d). D_i^{VP} and D_i^{VQ} are used to quantify the contribution of unit increment of net power at node i to nodal voltage. As shown in (7.a), it is linearly related to the electrical distance between a node and the source node.

$$\begin{aligned} D_i^{\text{VP}} &= \partial\Delta V_{i,t}/\partial P_{i,t}^{\text{bus}} = \sum_{l\in\xi(i)}\sum_{i=k+1}^{N_{\text{n}}} r_l M_{l-i} \\ D_i^{\text{VQ}} &= \partial\Delta V_{i,t}/\partial Q_{i,t}^{\text{bus}} = \sum_{l\in\xi(i)}\sum_{i=k+1}^{N_{\text{n}}} x_l M_{l-i} \end{aligned} \quad (7.a)$$

2) Branch transfer sensitivity

Branch transfer sensitivity is the derivative of the nodal net power to power flow of branches (6.c). It reflects the impact of unit increment of nodal net power on branch flexibility. B_{l-i}^{PP}, B_{l-i}^{QQ}, B_{l-i}^{PQ} and B_{l-i}^{QP} quantify the occupancy of a branch's power flow by the unit increment of node flexibility during spatial transfer. As shown in (7.b), it is linearly related to the topological connection between branches and nodes.

$$\begin{aligned} B_{l-i}^{\text{PP}} &= \partial P_{l,t}/\partial P_{i,t}^{\text{bus}} = M_{l-i},\ \ B_{l-i}^{\text{PQ}} = \partial P_{l,t}/\partial Q_{i,t}^{\text{bus}} = 0 \\ B_{l-i}^{\text{QQ}} &= \partial Q_{l,t}/\partial Q_{i,t}^{\text{bus}} = M_{l-i},\ \ B_{l-i}^{\text{QP}} = \partial Q_{l,t}/\partial P_{i,t}^{\text{bus}} = 0 \end{aligned} \quad (7.b)$$

3) Network loss sensitivity

Network loss sensitivity is the derivative of the nodal net power to network loss equation (6.e). L_i^{PP}, L_i^{PQ}, L_i^{QP} and L_i^{QQ} represent the contribution ratios of transfer expense during the spatial transfer of net power at a node. As shown in (7.c), it is linearly related to the branch transfer sensitivity factor.

$$\begin{aligned} L_i^{\mathrm{PP}} &= \partial P_t^{\mathrm{loss}} / \partial P_{i,t}^{\mathrm{bus}} = \textstyle\sum_{l\in\Omega_{\mathrm{b}}} 2r_l \cdot P_{l,t}^{*} \cdot B_{l-i}^{\mathrm{PP}} \\ L_i^{\mathrm{PQ}} &= \partial P_t^{\mathrm{loss}} / \partial Q_{i,t}^{\mathrm{bus}} = \textstyle\sum_{l\in\Omega_{\mathrm{b}}} 2r_l \cdot Q_{l,t}^{*} \cdot B_{l-i}^{\mathrm{QQ}} \\ L_i^{\mathrm{QP}} &= \partial Q_t^{\mathrm{loss}} / \partial P_{i,t}^{\mathrm{bus}} = \textstyle\sum_{l\in\Omega_{\mathrm{b}}} 2x_l \cdot P_{l,t}^{*} \cdot B_{l-i}^{\mathrm{PP}} \\ L_i^{\mathrm{QQ}} &= \partial Q_t^{\mathrm{loss}} / \partial Q_{i,t}^{\mathrm{bus}} = \textstyle\sum_{l\in\Omega_{\mathrm{b}}} 2x_l \cdot Q_{l,t}^{*} \cdot B_{l-i}^{\mathrm{QQ}} \end{aligned} \tag{7.c}$$

where $V_{i,t}$ is assumed to be approximate to 1 for linearization.

Flexibility sensitivity factors correlate nodal net power with the three flexibility aspects. Based on the analytic framework with flexibility sensitivity factors, the flexibility value of nodal net power is quantified in the form of price in the next section.

Remark: Power is a basic physical quantify in distribution networks and its distribution in space and time affects system operation. By contrast, operational flexibility is an inherent multi-dimensional property of distribution networks. Operational flexibility reflects the ability of distribution networks to maintain the stable, economic, and reliable operation of the entire system.

Operational flexibility analysis is aimed at adapting the distribution network to complex operating environments through analyzing the comprehensive impacts of power balance, power transfer, and power reserve on system operation. Also, operational flexibility analysis should satisfy diversified requirements of distribution networks, such as optimal operation and market clearing, etc., without violating various operational constraints in distribution networks. Based on power flow analysis, operational flexibility contains more evaluation and guidance information for system operation rather than mere power dispatch instructions of flexible resources. As for its application, operational flexibility is generally presented in a concrete description of power so that can be finally used to adjust power and improve system operation.

III. DLMP-BASED FLEXIBILITY PRICING MODEL

The DLMP-based flexibility pricing model is proposed for FDNs in this section. Multiple flexible resources are considered and flexibility constraints are constructed linearly using flexibility sensitivity factors.

A. Objective Function

The objective is to maximize social welfare, which is equivalent to minimizing the total operational flexibility cost in this paper. As shown in (8.a), the total cost is the sum of the costs for dispatching flexible resources C^{FR}, penalizing voltage flexibility shortage C^{V}, interacting aggregated flexibility with the external grid C^{sub}, and flexibility reserve C^{res}.

$$\min C = C^{\mathrm{FR}} + C^{\mathrm{V}} + C^{\mathrm{sub}} + C^{\mathrm{res}} \tag{8.a}$$

The cost C^{FR} is shown in (8.b). The flexible resources are with flexible power adjustment ability, represented by inverter-based DG, SOP, ESS, and DL. Detailed explanations are provided in Section IV.B. Flexible resources will respond to the fluctuating prices to satisfy flexible operation requirements. Moreover, flexible resources can provide flexibility services to improve system operational flexibility.

$$C^{\mathrm{FR}} = \textstyle\sum_{t\in\Omega_{\mathrm{T}}} \sum_{i\in\Omega_{\mathrm{FR}}^{\mathrm{P}}} (\sigma_{i,t}^{\mathrm{P}} P_{i,t}^{\mathrm{FR}} + \sum_{i\in\Omega_{\mathrm{FR}}^{\mathrm{Q}}} \sigma_{i,t}^{\mathrm{Q}} \left| Q_{i,t}^{\mathrm{FR}} \right|) \tag{8.b}$$

where $\Omega_{\mathrm{FR}}^{\mathrm{P}} = \Omega_{\mathrm{DL}} \cup \Omega_{\mathrm{SOP}} \cup \Omega_{\mathrm{ESS}}$ and $\Omega_{\mathrm{FR}}^{\mathrm{Q}} = \Omega_{\mathrm{DG}} \cup \Omega_{\mathrm{DL}} \cup \Omega_{\mathrm{SOP}} \cup \Omega_{\mathrm{ESS}}$ in this paper.

The desired nodal voltage flexibility (2.b) is converted to the penalty cost of voltage deviation based on the value of loss load (VoLL), as shown in (8.c). The penalty will reach the maximum $\sigma^{\mathrm{V}} P_{i,t}$ if the nodal voltage exceeds the secure range (2.a). The punishment cost is linearly approximate to the nodal net power if the nodal voltage is beyond the desired range (2.b) but within the secure range (2.a).

$$\begin{aligned} C^{\mathrm{V}} &= \textstyle\sum_{t\in\Omega_{\mathrm{T}}} \sum_{i\in\Omega_{\mathrm{n}}} \sigma^{\mathrm{V}} g(V_{i,t}) P_{i,t}^{\mathrm{TL}} \\ g(V_{i,t}) &= \begin{cases} 1 & , V_{i,t} \ge V_{\max}, V_{i,t} \le V_{\min} \\ \frac{V_{i,t} - \bar{V}_{\mathrm{flx}}}{V_{\max} - \bar{V}_{\mathrm{flx}}}, & \bar{V}_{\mathrm{flx}} < V_{i,t} < V_{\max} \\ \frac{\underline{V}_{\mathrm{flx}} - V_{i,t}}{\underline{V}_{\mathrm{flx}} - V_{\min}}, & V_{\min} < V_{i,t} < \underline{V}_{\mathrm{flx}} \\ 0 & , \underline{V}_{\mathrm{flx}} \le V_{i,t} \le \bar{V}_{\mathrm{flx}} \end{cases} \end{aligned} \tag{8.c}$$

where the penalty price factor σ^{V} is set based on the development status of users [38].

In addition, network aggregation flexibility is evaluated using the interaction cost of power purchased from the upper grid in (8.d) and the reserve cost of power flexibility in (8.e).

$$C^{\mathrm{sub}} = C^{\mathrm{sub,P}} + C^{\mathrm{sub,Q}} = \textstyle\sum_{t\in\Omega_{\mathrm{T}}} (\sigma_{\mathrm{s},t}^{\mathrm{P}} \cdot P_t^{\mathrm{sub}} + \sigma_{\mathrm{s},t}^{\mathrm{Q}} \cdot Q_t^{\mathrm{sub}}) \tag{8.d}$$

$$C^{\mathrm{res}} = \textstyle\sum_{t\in\Omega_{\mathrm{T}}} \sum_{i\in\Omega_{\mathrm{res}}} \sigma_{i,t}^{\mathrm{R}} (R_{i,t}^{\mathrm{up}} + R_{i,t}^{\mathrm{down}}) \tag{8.e}$$

where $\Omega_{\mathrm{res}} = \Omega_{\mathrm{ESS}} \cup \Omega_{\mathrm{DL}}$ and the upward and downward flexibility reserves are assumed to be at the same price $\sigma_{i,t}^{\mathrm{R}}$.

B. Sensitivity-based Node Flexibility Constraints

Using flexibility sensitivity factors, flexibility constraints can be represented by a set of linear equations w.r.t nodal net power as follows.

1) Nodal net power constraints

The nodal net power is the power summation of devices integrated into a node, as shown in (1). With advanced power electronics, flexible resources with two-quadrant or four-quadrant power controllable characteristics [39] are integrated into the source, network, and demand sides of FDNs.

On the source side, PVs and WTs as the inverter-based DGs are considered to be integrated into the system. To guarantee DG penetration, the active power curtailment is not considered and the reactive power of DGs can be adjusted. On the network side, the flexible resources can be classified into the spatial-transfer devices represented by SOP, and temporal-transfer devices represented by ESS [8]. SOP and ESS as typical network-side resources are considered to be integrated. On the demand side, DL which is delay-tolerant, and TL which is the fixed load as two typical load types are considered. Detailed operation constraints are listed in Appendix B.

2) Nodal voltage flexibility constraint

Secure voltage range (2.a) can be converted to following functions. Similarly, voltage deviation punishment (8.c) can be converted to linear functions of nodal net power.

$$\begin{aligned} &V_{\min} \le 1 - \left[D_i^{\mathrm{VP}}\left(P_{i,t}^{\mathrm{bus}} + F_{i,t}^{\mathrm{P}}\right) + D_i^{\mathrm{VQ}}\left(Q_{i,t}^{\mathrm{bus}} + F_{i,t}^{\mathrm{Q}}\right)\right] \ (\mu_i^{\mathrm{v},-}) \\ &1 - \left[D_i^{\mathrm{VP}}\left(P_{i,t}^{\mathrm{bus}} + F_{i,t}^{\mathrm{P}}\right) + D_i^{\mathrm{VQ}}\left(Q_{i,t}^{\mathrm{bus}} + F_{i,t}^{\mathrm{Q}}\right)\right] \le V_{\max} \ (\mu_i^{\mathrm{v},+}) \end{aligned} \tag{9}$$

3) Flexibility reserve constraints of flexible resources

The flexible resources with the charging/discharging capacity, represented by ESS and DL, can provide active power reserve as flexibility reserve [40]. The margin of flexibility reserve is constrained by power and SOC, as shown in Fig. 2.

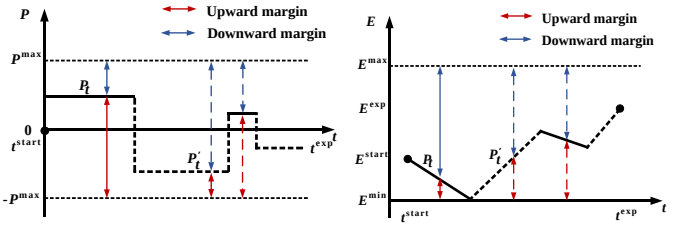

a) Power range constraint b) SOC range constraint

Fig. 2 Illustration of flexibility reserve margin limited by power and SOC.

(1) Reserve constraints of ESS

The margin of ESS flexibility reserve is shown in (10).

$$R_{i,t}^{\mathrm{ESS,up}} \le \min\left\{\bar{P}_i^{\mathrm{ESS}}, \bar{P}_{i,t}^{\mathrm{ESS,d}}\right\} - P_{i,t}^{\mathrm{ESS}}, \tag{10.a}$$

$$R_{i,t}^{\mathrm{ESS,down}} \le P_{i,t}^{\mathrm{ESS}} - \max\left\{-\bar{P}_i^{\mathrm{ESS}}, \bar{P}_{i,t}^{\mathrm{ESS,c}}\right\} \tag{10.b}$$

$$\bar{P}_{i,t}^{\mathrm{ESS,c}} + A_i^{\mathrm{E,L}}\left|\bar{P}_{i,t}^{\mathrm{ESS,c}}\right| = \left(E_{i,t-1}^{\mathrm{ESS}} - \bar{E}_i^{\mathrm{ESS}}\right)/\Delta t \tag{10.c}$$

$$\bar{P}_{i,t}^{\mathrm{ESS,d}} + A_i^{\mathrm{E,L}}\left|\bar{P}_{i,t}^{\mathrm{ESS,d}}\right| = \left(E_{i,t-1}^{\mathrm{ESS}} - \underline{E}_i^{\mathrm{ESS}}\right)/\Delta t \tag{10.d}$$

The maximum discharging power is non-negative ($\bar{P}_{i,t}^{\mathrm{ESS,d}} \ge 0$) and the maximum charging power is non-positive ($\bar{P}_{i,t}^{\mathrm{ESS,c}} \le 0$). Constraints (10.c)-(10.d) can be further converted to:

$$\bar{P}_{i,t}^{\mathrm{ESS,c}} = \frac{E_{i,t-1}^{\mathrm{ESS}} - \bar{E}_i^{\mathrm{ESS}}}{\left(1 - A_i^{\mathrm{E,L}}\right)\Delta t}, \ \bar{P}_{i,t}^{\mathrm{ESS,d}} = \frac{E_{i,t-1}^{\mathrm{ESS}} - \underline{E}_i^{\mathrm{ESS}}}{\left(1 + A_i^{\mathrm{E,L}}\right)\Delta t} \tag{10.e}$$

Note that reactive power of ESS is not considered in reserve constraints for simplicity, and will be investigated in the future.

(2) Reserve constraints of DL

Similarly to (10), the reserve constraints of DL are formulated in (11). Note that DL can only be charged.

$$\begin{aligned} &R_{i,t}^{\mathrm{DL,down}} \le \min\left\{\bar{P}_i^{\mathrm{DL}}, \bar{P}_{i,t}^{\mathrm{DL,c}}\right\} - P_{i,t}^{\mathrm{DL}}, \\ &R_{i,t}^{\mathrm{DL,up}} \le P_{i,t}^{\mathrm{DL}} - \max\left\{0, \underline{P}_{i,t}^{\mathrm{DL,c}}\right\} \qquad t \ge T_{i,\mathrm{st}}^{\mathrm{DL}} \end{aligned} \tag{11.a}$$

$$\begin{aligned} &\bar{P}_{i,t}^{\mathrm{DL,c}} = \frac{\bar{E}_i^{\mathrm{DL}} - E_{i,t-1}^{\mathrm{DL}}}{\Delta t}, \underline{P}_{i,t}^{\mathrm{DL,c}} = \frac{\underline{E}_i^{\mathrm{DL}} - E_{i,t-1}^{\mathrm{DL}}}{\Delta t} \\ &R_{i,t}^{\mathrm{DL,up}} = 0, \quad R_{i,t}^{\mathrm{DL,down}} = 0, \qquad 0 \le t \le T_{i,\mathrm{st}}^{\mathrm{DL}} \end{aligned} \tag{11.b}$$

C. Sensitivity-based Branch Flexibility Constraints

$$\begin{aligned} &\alpha_{c,0}\textstyle\sum_{i=k+1}^{N_{\mathrm{n}}} B_{l-i}^{\mathrm{PP}}\left(P_{i,t}^{\mathrm{bus}} + F_{i,t}^{\mathrm{P}}\right) + \alpha_{c,1}\sum_{i=k+1}^{N_{\mathrm{n}}}\left(B_{l-i}^{\mathrm{QQ}} Q_{i,t}^{\mathrm{bus}} + \right. \\ &\left. + F_{i,t}^{\mathrm{Q}}\right) + \alpha_{c,2} S_l \le 0, \forall c \in \{1,2,\ldots,12\}, \forall l: L_k \in \Omega_{\mathrm{b}} \ \ (\mu_{l,c}) \end{aligned} \tag{12}$$

To express the linear correlation, the branch transfer factor is used. To linearize the quadratic term in (3.a), the approximate polygon method [37] is adopted. The sensitivity factor-based branch flexibility constraint is shown in (12).

D. Sensitivity-based Network Flexibility Constraints

1) Network aggregated flexibility constraints

The original expression (4) can be converted to the linear constraint (13) using network loss sensitivity factors.

$$\begin{aligned} &P_t^{\mathrm{sub}} - \textstyle\sum_{i\in\Omega_{\mathrm{n}}}\left(1 + L_i^{\mathrm{PP}}\right)P_{i,t}^{\mathrm{bus}} - \sum_{i\in\Omega_{\mathrm{n}}} L_i^{\mathrm{PQ}} Q_{i,t}^{\mathrm{bus}} + P_t^{\mathrm{loss}} = 0 \quad (\lambda^{\mathrm{P}}) \\ &Q_t^{\mathrm{sub}} - \textstyle\sum_{i\in\Omega_{\mathrm{n}}}\left(1 + L_i^{\mathrm{QQ}}\right)Q_{i,t}^{\mathrm{bus}} - \sum_{i\in\Omega_{\mathrm{n}}} L_i^{\mathrm{QP}} P_{i,t}^{\mathrm{bus}} + Q_t^{\mathrm{loss}} = 0 \quad (\lambda^{\mathrm{Q}}) \end{aligned} \tag{13}$$

2) Network flexibility reserve constraints

As formulated in (5.c). To linearize the absolute term, auxiliary variable $\hat{R}_t^{\mathrm{res}}$ is introduced to convert (5.c) as follows:

$$\begin{aligned} &\hat{R}_t^{\mathrm{res}} \ge \beta \textstyle\sum_{i\in\Omega_{\mathrm{n}}} P_{i,t}^{\mathrm{bus}} \ (\mu_i^{\mathrm{R1}}) \\ &\hat{R}_t^{\mathrm{res}} \ge -\beta \textstyle\sum_{i\in\Omega_{\mathrm{n}}} P_{i,t}^{\mathrm{bus}} \ (\mu_i^{\mathrm{R2}}) \\ &\textstyle\sum_{i\in\Omega_{\mathrm{res}}}\left(R_{i,t}^{\mathrm{up}} + R_{i,t}^{\mathrm{down}}\right) \ge \hat{R}_t^{\mathrm{res}} \end{aligned} \tag{14}$$

IV. Solution and Decomposition of Flexibility Price

This section provides the solution methodology of flexibility pricing model and analyzes flexibility price.

A. Solution of Flexibility Pricing Model

The flexibility pricing model is an LP problem, which guarantees that the local optimum is the global optimum. To express its dual problem, the proposed LP model is transformed into a Lagrange duality problem. The compact form is in (15) and the expression of Lagrangian function $L(\boldsymbol{x}, \boldsymbol{\lambda}, \boldsymbol{\mu})$ is provided in (16).

$$\begin{aligned} &\max \psi(\boldsymbol{\lambda}, \boldsymbol{\mu}) = \max_{\boldsymbol{\lambda},\boldsymbol{\mu}} \inf_{\boldsymbol{x}} \left[L(\boldsymbol{x}, \boldsymbol{\lambda}, \boldsymbol{\mu})\right] = \max_{\boldsymbol{\lambda},\boldsymbol{\mu}} \min_{\boldsymbol{x}} L(\boldsymbol{x}, \boldsymbol{\lambda}, \boldsymbol{\mu}) \\ &\text{s.t. } \boldsymbol{\mu} \ge 0 \end{aligned} \tag{15}$$

where $\boldsymbol{x}$ is the vector of control variables, including the active power and reactive power of flexible resources. $\boldsymbol{\lambda}$ and $\boldsymbol{\mu}$ are the vectors of Lagrange multipliers of flexibility constraints.

DLMP at node i is the first-order partial derivative of (16) to the nodal net active and reactive power. According to duality analysis, the DLMP-based flexibility price comprises products of different flexibility sensitivity factors and shadow price which is the Lagrange multiplier of related flexibility constraints when primal model reaches its optimum.

The proposed model can be solved by a commercial solver, such as CPLEX or MOSEK [41]. The optimal dispatch strategy $\boldsymbol{x}^*$ can be obtained and the DLMP-based flexibility price of nodal net power related to strategy $\boldsymbol{x}^*$ is revealed in (17).

B. Decomposition of Flexibility Price

Based on the analytic framework for flexibility quantification, the DLMP-based flexibility price can be viewed as the summation of the node integration, branch transfer, and network aggregation price components, as shown in (17.a). The flexibility price consists of flexibility sensitivity factors and Lagrange multipliers of flexibility constraints as well as the constant terms obtained by the first-order partial derivative of objective function C to nodal net power.

$$
\begin{aligned}
&L(\boldsymbol{x},\boldsymbol{\lambda},\boldsymbol{\mu}) = \\
&\textstyle\sum_{t\in\Omega_{\mathrm{T}}}\{C-\mu_i^{\mathrm{v},-}\left[V_{\min}-1+D_i^{\mathrm{VP}}\left(P_{i,t}^{\mathrm{bus}}+F_{i,t}^{\mathrm{P}}\right)+D_i^{\mathrm{VQ}}\left(Q_{i,t}^{\mathrm{bus}}+F_{i,t}^{\mathrm{Q}}\right)\right]-\mu_i^{\mathrm{v},+}\left[1-D_i^{\mathrm{VP}}\left(P_{i,t}^{\mathrm{bus}}+F_{i,t}^{\mathrm{P}}\right)-D_i^{\mathrm{VQ}}\left(Q_{i,t}^{\mathrm{bus}}+F_{i,t}^{\mathrm{Q}}\right)-V_{\max}\right] \\
&-\textstyle\sum_{l\in\Omega_{\mathrm{b}}}\sum_{c=1}^{12}\mu_{l,c}\left[\alpha_{c,0}\sum_{i=k+1}^{N_{\mathrm{n}}}B_{l-i}^{\mathrm{PP}}\left(P_{i,t}^{\mathrm{bus}}+F_{i,t}^{\mathrm{P}}\right)+\alpha_{c,1}\sum_{i=k+1}^{N_{\mathrm{n}}}B_{l-i}^{\mathrm{QQ}}\left(Q_{i,t}^{\mathrm{bus}}+F_{j,t}^{\mathrm{Q}}\right)+\alpha_{c,2}S_l\right] \\
&-\lambda^{\mathrm{P}}\left[\textstyle\sum_{i\in\Omega_{\mathrm{n}}}\left(1+L_i^{\mathrm{PP}}\right)P_{i,t}^{\mathrm{bus}}+\sum_{i\in\Omega_{\mathrm{n}}}L_i^{\mathrm{PQ}}Q_{i,t}^{\mathrm{bus}}-P_t^{\mathrm{loss}}-P_t^{\mathrm{sub}}\right]-\lambda^{\mathrm{Q}}\left[\textstyle\sum_{i\in\Omega_{\mathrm{n}}}\left(1+L_i^{\mathrm{QQ}}\right)Q_{i,t}^{\mathrm{bus}}+\sum_{i\in\Omega_{\mathrm{n}}}L_i^{\mathrm{QP}}P_{i,t}^{\mathrm{bus}}-Q_t^{\mathrm{loss}}-Q_t^{\mathrm{sub}}\right] \\
&-\mu_i^{\mathrm{R1}}\left(\beta\textstyle\sum_{i\in\Omega_{\mathrm{n}}}P_{i,t}^{\mathrm{bus}}-\hat{R}_t^{\mathrm{res}}\right)-\mu_i^{\mathrm{R2}}\left(-\beta\textstyle\sum_{i\in\Omega_{\mathrm{n}}}P_{i,t}^{\mathrm{bus}}-\hat{R}_t^{\mathrm{res}}\right) \\
&-\lambda_i^{\mathrm{Pbus}}\left[P_{i,t}^{\mathrm{bus}}-P_{i,t}^{\mathrm{TL}}-P_{i,t}^{\mathrm{DL}}+P_{i,t}^{\mathrm{DG}}+P_{i,t}^{\mathrm{ESS}}+P_{i,t}^{\mathrm{SOP}}\right]-\lambda_i^{\mathrm{Qbus}}[Q_{i,t}^{\mathrm{bus}}-Q_{i,t}^{\mathrm{TL}}-Q_{i,t}^{\mathrm{DL}}+Q_{i,t}^{\mathrm{DG}}+Q_{i,t}^{\mathrm{ESS}}+Q_{i,t}^{\mathrm{SOP}}]\}
\end{aligned}
\tag{16}
$$

1) Node integration price $\pi_{i,t}^{P,Bus}+\pi_{i,t}^{Q,Bus}$

As expressed in (17.b) and (17.c), it quantifies the value of net power at node i to nodal voltage flexibility. Linear combination of Lagrange multipliers w.r.t nodal voltage flexibility constraints, $\left(\mu_i^{\mathrm{v},-}-\mu_i^{\mathrm{v},+}\right)$, is the unit change of marginal node voltage flexibility cost caused by the unit change of nodal net power. $\lambda_i^{\mathrm{Pbus}}-\sigma_{i,t}^{\mathrm{P}}I_{i,t}^{\mathrm{FR,P}}-\sigma^{\mathrm{V}}g(V_{i,t})$ and $\lambda_i^{\mathrm{Qbus}}-\sigma_{i,t}^{\mathrm{P}}I_{i,t}^{\mathrm{FR,Q}}$ are the linear combinations of Lagrange multipliers of nodal net power constraints and nodal-level requirements in objective function. It reflects the impact of diversified flexible requirements on the nodal net power in the form of price, as nodal net power is the basic unit to realize the balance of differentiated flexible services. Various flexible resources are standardized and coordinated on the nodal net power.

2) Branch transfer price $\pi_{i,t}^{P,Bran}+\pi_{i,t}^{Q,Bran}$

It quantifies the efficient and secure transfer through branches for dispatch of node integration flexibility. In (17.d) and (17.e), the linear combination of Lagrange multipliers w.r.t branch transfer flexibility constraints, $\sum_{c=1}^{12}\mu_{l,c}$, quantifies the value of nodal net power to branch flexibility. The linear combinations of sensitivity factors $\sum_{c=1}^{12}\alpha_{c,0}B_{i-i}^{\mathrm{PP}}$ and $\sum_{c=1}^{12}\alpha_{c,1}B_{i-i}^{\mathrm{QQ}}$ quantify the impact ratios of nodal net power to the spatial-transfer ability of branch flexibility. The flexibility transfer expenses during branch transfer to aggregate power interacted with external grids are quantified in the last two items in (17.d) and (17.e), respectively.

3) Network aggregation price $\pi_{i,t}^{P,Net}+\pi_{i,t}^{Q,Net}$

In (17.f)-(17.g), it reflects the impact of nodal net power on the interaction of aggregated flexibility with external grids and on the flexibility reserve. Linear combination of Lagrange multipliers w.r.t network flexibility reserve constraints, $(\mu_i^{\mathrm{R1}}-\mu_i^{\mathrm{R2}})$, quantifies the flexibility value of network flexibility reserve. Lagrange multipliers w.r.t network aggregation flexibility constraints, λ^{P} and λ^{Q}, indicate the flexibility price of aggregated power interacting with external grids. β denotes the impact ratio of nodal net power to network flexibility reserve. The constant terms $-\sigma_{\mathrm{s},t}^{\mathrm{P}}$, $-\sigma_{i,t}^{\mathrm{R}}$ and $-\sigma_{\mathrm{s},t}^{\mathrm{Q}}$ reflect the price impact of network-level flexible requirements in objective function on the nodal net power.

The nodal net active and reactive power are priced according to their spatial-temporal impact on operational flexibility. Each price component quantifies the impact of nodal net power at a node in different time slots on the related flexibility aspect of the entire FDN. As a result, the DLMP-based flexibility price can be utilized as an incentive signal for flexible resource dispatch. The proposed method of operational flexibility can further provide an explicit analytic solution to balance operational flexibility in FDNs.

$$
\begin{aligned}
\pi_{i,t}^{\mathrm{P}} &= \partial L/\partial P_{i,t}^{\mathrm{bus}} = \pi_{i,t}^{\mathrm{P,Bus}}+\pi_{i,t}^{\mathrm{P,Bran}}+\pi_{i,t}^{\mathrm{P,Net}} \\
\pi_{i,t}^{\mathrm{Q}} &= \partial L/\partial Q_{i,t}^{\mathrm{bus}} = \pi_{i,t}^{\mathrm{Q,Bus}}+\pi_{i,t}^{\mathrm{Q,Bran}}+\pi_{i,t}^{\mathrm{Q,Net}}
\end{aligned}
\tag{17.a}
$$

$$\pi_{i,t}^{\mathrm{P,Bus}} = D_i^{\mathrm{VP}}\left(\mu_i^{\mathrm{v},-}-\mu_i^{\mathrm{v},+}\right)+\lambda_i^{\mathrm{Pbus}}-\sigma_{i,t}^{\mathrm{P}}I_{i,t}^{\mathrm{FR,P}}-\sigma^{\mathrm{V}}g(V_{i,t}) \tag{17.b}$$

$$\pi_{i,t}^{\mathrm{Q,Bus}} = D_i^{\mathrm{VQ}}\left(\mu_i^{\mathrm{v},-}-\mu_i^{\mathrm{v},+}\right)+\lambda_i^{\mathrm{Qbus}}-\sigma_{i,t}^{\mathrm{P}}I_{i,t}^{\mathrm{FR,Q}} \tag{17.c}$$

$$\pi_{i,t}^{\mathrm{P,Bran}} = \textstyle\sum_{l\in\Omega_{\mathrm{b}}}\sum_{c=1}^{12}\mu_{l,c}\alpha_{c,0}\,B_{l-i}^{\mathrm{PP}}+L_i^{\mathrm{PP}}\lambda^{\mathrm{P}}+L_i^{\mathrm{QP}}\lambda^{\mathrm{Q}} \tag{17.d}$$

$$\pi_{i,t}^{\mathrm{Q,Bran}} = \textstyle\sum_{l\in\Omega_{\mathrm{b}}}\sum_{c=1}^{12}\mu_{l,c}\alpha_{c,1}\,B_{l-i}^{\mathrm{QQ}}+L_i^{\mathrm{QQ}}\lambda^{\mathrm{Q}}+L_i^{\mathrm{PQ}}\lambda^{\mathrm{P}} \tag{17.e}$$

$$\pi_{i,t}^{\mathrm{P,Net}} = \lambda^{\mathrm{P}}-\sigma_{\mathrm{s},t}^{\mathrm{P}}+\beta\left(\mu_i^{\mathrm{R1}}-\mu_i^{\mathrm{R2}}-\sigma_{i,t}^{\mathrm{R}}\right) \tag{17.f}$$

$$\pi_{i,t}^{\mathrm{Q,Net}} = \lambda^{\mathrm{Q}}-\sigma_{\mathrm{s},t}^{\mathrm{Q}} \tag{17.g}$$

where $I_{i,t}^{\mathrm{FR,P}}=I_{i,t}^{\mathrm{FR,Q}}=0$, if the node is without flexible resources. At nodes with flexible resources, if controllable resources are load-type, then $I_{i,t}^{\mathrm{FR,P}}=1$, else $I_{i,t}^{\mathrm{FR,P}}=-1$; if the optimal dispatch is to inject reactive power, then $I_{i,t}^{\mathrm{FR,Q}}=-1$, else $I_{i,t}^{\mathrm{FR,Q}}=1$.

Remark: In addition to flexibility dispatch, there are several promising applications of the DLMP-based flexibility price. First, various flexibility services can be classified and priced under the proposed analytic framework. DLMP-based flexibility pricing can be applied in the peer-to-peer trading of operational flexibility in distribution networks. Second, the DLMP-based flexibility analysis can be applied in the allocation of flexible resources to enhance operational flexibility of FDNs.

V. Case Studies and Analysis

The effectiveness of the proposed quantification and analysis method of operational flexibility is verified on a modified IEEE 33-node test case and a modified IEEE 123-node test case. The proposed model is implemented in the YALMIP optimization toolbox [42] with MATLAB R2019b and solved by IBM ILOG CPLEX 12.10. The numerical experiments were carried out on a computer with an Intel Xeon CPU E5-1620 processor running at 3.70 GHz and 32 GB of RAM.

A. Modified IEEE 33-node Test Case

The test case is based on a modified IEEE 33-node distribution system, as shown in Fig. 3. It includes a substation and 32 branches, of which the rated voltage level is 12.66 kV. Total active power and reactive power demands are 3.715 MW and 2.300 Mvar. The detailed parameters are shown in [8].

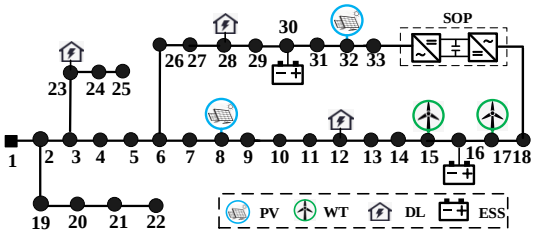

Fig. 3. Structure of the modified IEEE 33-node test case.

To incorporate the impact of DG fluctuation, two PV units and two WT units are integrated into the network, as shown in Table I. The daily DG and load operation curves are given in Fig. 4, taking 1 hour as the time resolution. An SOP is installed between Node 18 and Node 33. Considering the high efficiency of power electronic-based inverters, the power loss coefficient of each inverter is set to 0.02. The detailed parameters of ESSs and DLs are listed in Tables II and III, respectively.

The secure voltage range is set as 0.90-1.10 p.u.. The desired voltage range is set as 0.97-1.03 p.u., which can be adjusted based on the requirements of DSOs. The time of use (TOU) tariff is depicted in Fig. 5 and the price parameters are listed in Table IV. Set the reserve ratio β =10%.

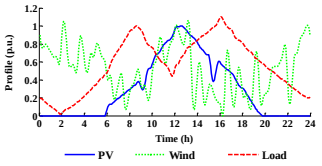

Fig. 4. Operation curves of DG and load.

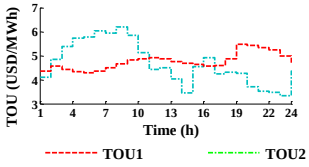

Fig. 5. Price curves.

TABLE I

INSTALLATION PARAMETERS OF DGS

Type	Node	Maximum active power/MW	Capacity/MWp(MVA)
PV	8	0.5	0.6
	32	0.5	0.6
WT	15	0.8	1.0
	17	1.0	1.2

TABLE II

INSTALLATION PARAMETERS OF ESSS

Node	Active power/kW	Reactive power/kvar	SOC_0/kWh	SOC/kWh
16, 30	[-600, 600]	[-600, 600]	300	[100, 900]

TABLE III

INSTALLATION PARAMETERS OF DLS

Node	Active power/kW	T_{start}/h	T_{req}/h	SOC_0/kWh	SOC_{req}/kWh	ϑ^{DL}
12	[0, 100]	1	8	30	200	
23	[0, 400]	1	8	100	400	0.9
28	[0, 400]	16	24	100	400	

TABLE IV

PRICE PARAMETERS

Type	Amount/(USD/MWh)
Active power from upper grid $\sigma^{P}_{s,t}$	TOU 1
Reactive power from upper grid $\sigma^{Q}_{s,t}$	0.1* TOU 1
Voltage deviation punishment σ^{V}	5.25
Reactive power from flexible devices $\sigma^{Q}_{i,t}$	0.1* TOU 1
Active power schedule of flexible devices $\sigma^{P}_{i,t}$	TOU 1
Active power reserve of flexible devices $\sigma^{R}_{i,t}$	TOU 2

B. *Analysis of Flexibility Price*

The results of flexibility price are analyzed to quantify the flexibility value of nodal net power in this section. The flexibility price of nodal active and reactive power in the FDN are respectively depicted in Fig. 6(a) and Fig. 6(b). Note that to export power to a node is assumed the positive direction.

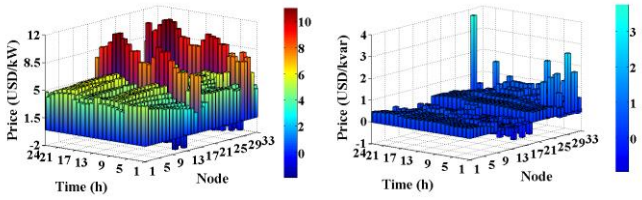

(a) Active power price (b) Reactive power price

Fig. 6 Price signals of nodes in a day.

1) *Comprehensive flexibility price*

The flexibility price quantifies the comprehensive impact of nodal net power on node integration, branch transfer, and network aggregation flexibility properties. As illustrated in Fig. 6, there is an obvious price variation with nodes and time slots.

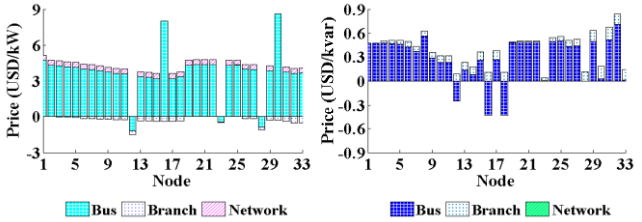

(a) Flexibility price for $P^{bus}_{i,t}$ at 12:00 (b) Flexibility price for $Q^{bus}_{i,t}$ at 12:00

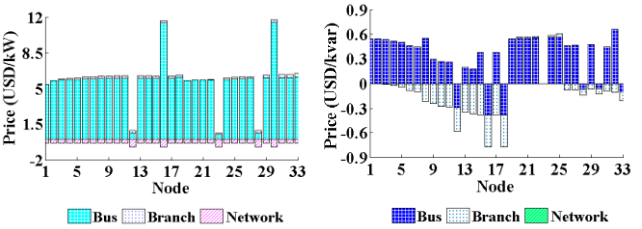

(c) Flexibility price for $P^{bus}_{i,t}$ at 19:00 (d) Flexibility price for $Q^{bus}_{i,t}$ at 19:00

Fig. 7 Flexibility price at 12:00 and 19:00.

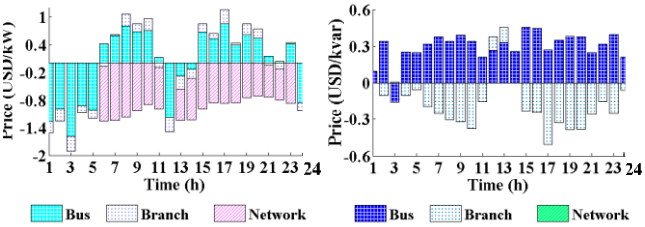

(a) Active power price of Node 12 (b) Reactive power price of Node 17

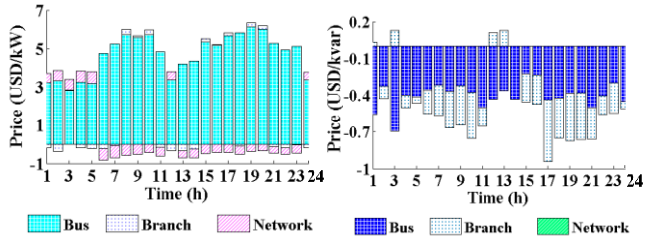

(c) Active power price of Node 18 (d) Reactive power price of Node 18

Fig. 8 Flexibility price of some nodes.

The flexibility price in some time slots is further displayed in Fig. 7. The flexibility price results of Nodes 17 and 33 in a day are depicted in Fig. 8. As displayed, the flexibility price at the same time varies with nodes. The price proportions at a node vary with time slots due to various occupancy of the three flexibility aspects. The price variation illustrates that there exist obvious spatial-temporal differences in the impacts of nodal net power on operational flexibility in FDNs.

Note that a positive flexibility price means that net power consumption will be charged and net power injection will be paid, while a negative price implies payment for power consumption or an income for power injection. The flexibility price also reflects different power dispatch schemes at each location to realize the same worth of flexibility service. That is, at nodes with a very small price, a large power dispatch may have only a little influence on operational flexibility cost. While the same influence can be achieved by a small net power at nodes with a large absolute price value.

Then, flexibility price components are further analyzed from the perspective of operational flexibility.

2) Node flexibility price

Figs. 9(a)-(b) illustrate the node flexibility price. It can be seen node flexibility price at most nodes is positive, thereby power exports will be charged. Also, the price component exists a negative value which indicates that to increase nodal power export or to decrease nodal power injection is motivated to prevent the lack of nodal integration flexibility.

The nodal integration flexibility of the FDN is more sensitive to the net power at nodes with a large absolute value of node flexibility price. For example, if the node with a positive node flexibility price has a relatively large net active power export, insufficient node integration flexibility may occur represented by over-low nodal voltage. Generally, nodes with flexible resources have a higher absolute value of price than other nodes. Flexible resources will be motivated to adjust active and reactive power to improve comprehensive operational performance.

However, an over-large net active power injection may lead to another extreme of flexibility lack such as over-high nodal voltage. That is, a node with proper net power dispatch facilitates the improvement of node integration flexibility. Also, it requires branch transfer to further balance the local flexibility.

3) Branch flexibility price

Figs. 9(c)-(d) depict the branch flexibility price. Similarly, the branch transfer flexibility of FDNs is more sensitive to the nodes with a large absolute value of branch flexibility price. Similarly, the negative price at some nodes indicates that net power export is motivated in case of the lack of branch transfer flexibility such as branch congestion. As for the positive price, a larger value means that the node is more motivated to inject power for branch transfer flexibility improvement.

The branch flexibility price at 12:00 is marked with a red box in Figs. 9(c)-(d). The absolute value of branch flexibility price increases with the nodes extending to the end of the feeder. At Nodes 8-18 and 25-33, the price of nodal net active power is negative and the price of nodal net reactive power is positive. Such a trend indicates that exporting active power and injecting reactive power are motivated at these nodes to improve branch transfer flexibility of the entire system. The branch flexibility price of nodal active power at Node 17 motivates an opposing power orientation with the node flexibility price, as shown in Fig. 8(b). It indicates that active power injection should not be too large especially when the reactive power injection is motivated because it is likely to cause branch congestion.

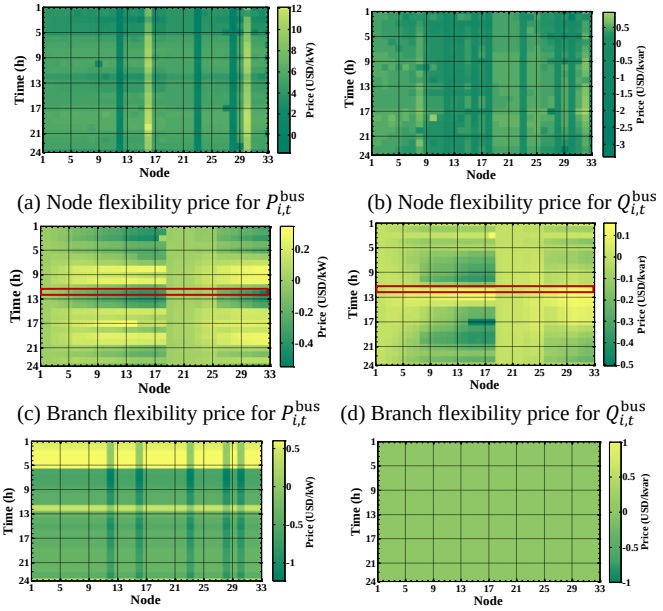

(a) Node flexibility price for $P_{i,t}^{\mathrm{bus}}$ (b) Node flexibility price for $Q_{i,t}^{\mathrm{bus}}$

(c) Branch flexibility price for $P_{i,t}^{\mathrm{bus}}$ (d) Branch flexibility price for $Q_{i,t}^{\mathrm{bus}}$

(e) Network flexibility price for $P_{i,t}^{\mathrm{bus}}$ (f) Network flexibility price for $Q_{i,t}^{\mathrm{bus}}$

Fig. 9 Heap maps of flexibility price components.

4) Network flexibility price

The network flexibility price is illustrated in Figs. 9(e)-(f). The network flexibility price is the sum of the interaction impact with the external grid and the reserve impact inside the system. This price component mainly varies with time. Nodes 12, 16, 23, 28, and 30 with devices to provide flexibility reserve are motivated to provide reserve by the price.

The power purchase price $\sigma_{\mathrm{s},t}^{\mathrm{P}}$, $\sigma_{\mathrm{s},t}^{\mathrm{Q}}$ and reserve price $\sigma_{i,t}^{\mathrm{P}}$ are respectively determined by the wholesale market and DSOs and only vary with time. As the pricing interaction with external grids is not considered in this paper, DLMPs of network aggregated flexibility at all nodes are equal to and offset the locational marginal price of power purchased from the external grids, as expressed in (19). Note that the impact of power purchase price from upper grid is also reflected in the node flexibility price at the source node through the impact quantification of nodal net power constraints. The node flexibility price of the source node can be expressed in the form of (20). The impact of pricing interaction among FDNs will be investigated in the future.

$$\lambda_{i,t}^{\mathrm{P}} = \sigma_{\mathrm{s},t}^{\mathrm{P}},\ \ \lambda_{i,t}^{\mathrm{Q}} = \sigma_{\mathrm{s},t}^{\mathrm{Q}} \tag{19}$$

$$\pi_{0,t}^{\mathrm{P,Bus}} = \sigma_{\mathrm{s},t}^{\mathrm{P}}, \pi_{0,t}^{\mathrm{Q,Bus}} = \sigma_{\mathrm{s},t}^{\mathrm{Q}} \tag{20}$$

Based on the above analysis, controllable devices can be motivated by the flexibility price to contribute to improving the system's operational benefits. Thus, the DLMP-based flexibility price could be an effective incentive for flexible resource dispatch to achieve a feasible balance of diversified flexibility requirements in FDNs.

C. Guide of Flexibility Price

Two scenarios are used to verify the effectiveness of the DLMP-based flexibility quantification and analysis method. The incentive effect of flexibility price on flexibility enhancement services is further elaborated with the illustration of system operation performance comparison.

Scenario I: There is no coordinated strategy for flexible resources in FDNs. The initial state is obtained under the TOU and without network-side resources SOP and ESS.

Scenario II: DLMP-based flexibility price is obtained to quantify the flexibility value, and is used to coordinate multiple resources for operational flexibility improvement of FDNs based on the proposed method.

Based on the proposed approach, Scenario II uses the DLMP-based flexibility price to dispatch flexible resources to provide operational flexibility services. The computational time is 137.21s for solving the daily DLMP-based flexibility price of the modified IEEE 33-node test case. Tables V and VI list the operation performance of the two scenarios.

TABLE V
OPERATION OBJECTIVES OF SCENARIOS I AND II

Scenario	$C^{\text{sub,P}}$ (USD)	$C^{\text{sub,Q}}$ (USD)	$C^{\text{FR,P}}$ (USD)	$C^{\text{FR,Q}}$ (USD)	C^{V} (USD)	C^{res} (USD)	Total (USD)
I	111.8747	16.1220	0	-	14.1535	-	142.1509
II	106.1767	4.3849	1.6908	5.1928	0.1702	12.5328	118.7094

Note that $C^{\text{FR,P}}$ is the cost of device losses and $C^{\text{FR,Q}}$ is the cost of reactive power services.

TABLE VI
PERFORMANCE COMPARISON OF SCENARIOS I AND II

Scenario	Total loss (kWh)	Network loss (kWh)	Device loss (kWh)	Maximum loading rate (%)	Voltage (p.u.)	Voltage deviation index (VDI)
I	1922.2	1922.2	-	168.54	0.9416-1.0828	0.0535
II	1446.5	1079.6	366.9	100	0.9700-1.0362	0.0004

In terms of flexibility costs, Scenario II has a less total flexibility cost and a 16.49% reduction in the power purchase payment to the upper grid than Scenario I, as shown in Table V. As flexible resources are guided to adjust reactive power locally, the voltage profile is improved and the payment for voltage deviation punishment is almost zero.

$$\text{VDI} = \frac{\sum_{t=1}^{N_\text{T}} \sum_{i=1}^{N_\text{n}} |V_{i,t} - \widetilde{V}_\text{flx}|}{N_\text{T} \cdot N_\text{n}} \ (V_{i,t} \geq \overline{V}_\text{flx} || V_{i,t} \leq \underline{V}_\text{flx}) \qquad (21)$$

In terms of flexibility performance, the distribution network in Scenario I has an obvious spatial-temporal unbalance of operational flexibility due to a lack of proper dispatch, as shown in Table VI. Contrarily, Scenario II uses the flexibility price to guide flexible resources. Scenario II has a 24.75% decrement in operation losses than Scenario I, in which the power loss is used to reflect the transfer expense. In addition, decreased power losses, improved voltage profiles and branch loading ratios show that it can effectively improve the uneven node flexibility and insufficient branch transfer flexibility.

1) Guide of node flexibility price

Fig. 10(a) illustrates system voltage extremes of the two Scenarios in a day. Fig. 10(b) further displays voltage profiles of Node 17 with a large electrical distance to the source node. Fig. 11 depicts the voltage profiles of all nodes in Scenario II. In Scenario I, there is a severely uneven spatial-temporal distribution of node integration flexibility. The main reason is the local power imbalance: From 0:00-5:00, 11:00-13:00, and 23:00-24:00, the active power injection of WT in Node 17 is larger than the adjacent loads' demands. From 7:00-9:00 and 15:00-17:00, loads are relatively heavy and PV in Node 32 cannot locally satisfy the power demands at Nodes 26-33.

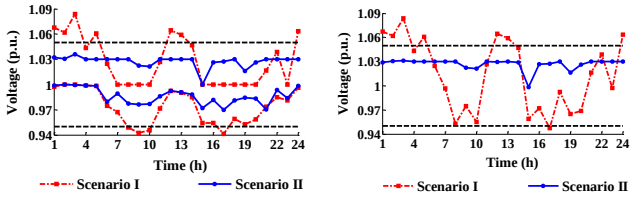

(a) All the nodes (b) Node 17

Fig. 10 Extreme voltage in Scenarios I and II.

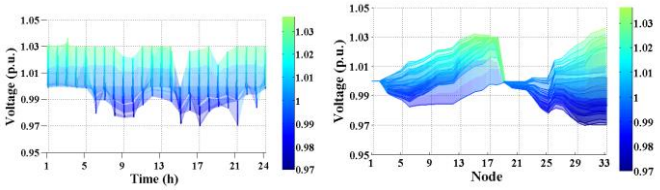

(a) Temporal voltage profiles (b) Nodal voltage profiles

Fig. 11 Nodal voltage profiles of Scenario II.

In Scenario II based on the proposed approach, the impact of nodal net power on nodal voltage flexibility is quantified as the nodal flexibility price. The available resources SOP, ESSs, DGs, and DLs are guided to support the nodes lacking node flexibility. As displayed in Fig. 11, voltage profiles at Nodes 15 and 17 are suppressed around the desired voltage range. The needed nodal voltage flexibility is transmitted to Nodes 30-33. Thus, voltage violations are significantly eliminated and voltage fluctuations are suppressed, as listed in Table VI.

2) Guide of branch flexibility price

Fig. 12 depicts the comparison of branch loading ratios in Scenarios I and II. Without coordination of flexible resources, Scenario I not only lacks node flexibility but also exists severe branch congestion, which hinders secure operation. In Fig. 12(a), severe congestion happens at 12:00 on Branches 6-14 in Scenario I due to the heavy active power injection of DGs.

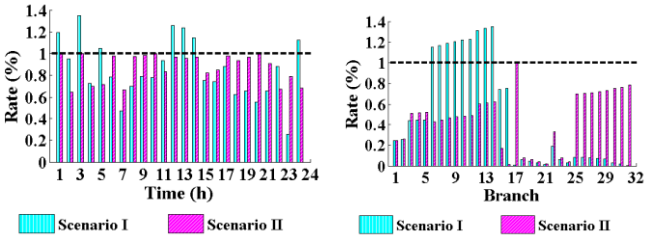

(a) Branch loading ratios in a day. (b) Branch loading ratios at 12:00

Fig. 12 Maximum Branch loading ratios of Scenarios I and II.

In Scenario II, flexible resources in the FDN, especially at Nodes 8-18 and 25-33, are motivated to guarantee the branch transfer flexibility is not harmed under the diversified flexibility requirements. As listed in Table VI, branch congestion is 100% mitigated in Scenario II. Taking 12:00 as an example, the redundant local active power at Nodes 15-18 is properly

transmitted to Node 33 by SOP. As shown in Fig. 12(b), congestion on Branches 6-14 is avoided with better usage of loading abilities of Branches 25-32.

3) Guide of network flexibility price

Flexible resources also respond to network flexibility price which aims to guide the entire system to economic operation with a certain reserve to cope with power fluctuations.

According to Table V, although the total power purchase payment is similar in Scenarios I and II, the flexibility reserve purchased in Scenario II can moderately enhance the response of FDNs to power fluctuations. In addition, compared with Scenario I, through the comprehensive guide of flexibility price, the dependence of FDNs on reactive power from the external grid is greatly reduced by 72.80% in Scenario II. There is also less reliance on external active power in Scenario II.

D. Test on Large System

The scalability to large-scale FDNs of the proposed approach is tested on a modified IEEE 123-node test case. Fig. 13 shows the topology of the test case. The rated voltage level is 10.5 kV. The total active and reactive power loads on the system are 4.885 MW and 2.710 Mvar. The detailed parameters are provided in [43].

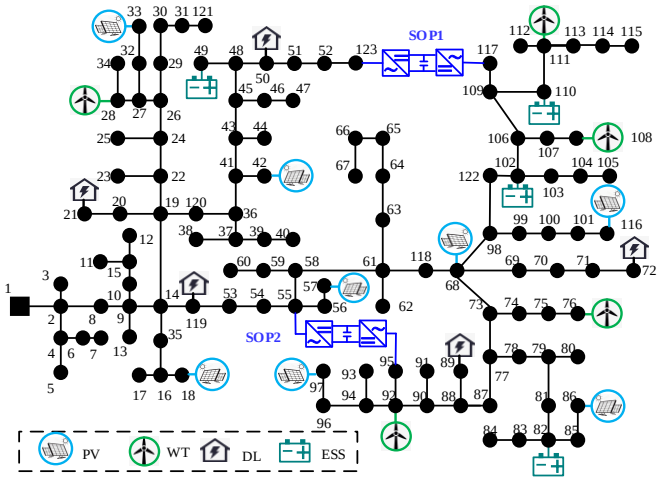

Fig. 13. Topology of the modified IEEE 123-node test case.

TABLE VII

INSTALLATION PARAMETERS OF ESSS

Node	Active power/kW	Reactive power/kvar	SOC_0/kWh	SOC/kWh
49	[-250, 250]	[-250,2 50]	300	[100, 600]
82	[-500, 500]	[-500, 500]	300	[100, 600]
102	[-300, 300]	[-300, 300]	300	[100, 600]
110	[-250, 250]	[-250, 250]	300	[100, 600]

TABLE VIII

INSTALLATION PARAMETERS OF DLS

Node	Active power/kW	T_{start}/h	T_{req}/h	SOC_0/kWh	SOC_{req}/kWh	ϑ^{DL}
21	[0, 100]	8	16	30	200	
50	[0, 100]	12	24	30	200	
72	[0, 400]	1	8	100	400	0.9
89	[0, 400]	16	24	100	400	
119	[0, 100]	16	24	30	200	

To fully consider the impact of DG integration, six PVs with 0.5 MWp capacity each and three WTs with 1.2 MVA capacity each are integrated into FDN. The maximum active power output of each PV and WT is 0.3 MW and 1.0 MW, respectively. In addition, four ESSs and five DLs are installed, as listed in Tables VII and VIII. Two SOPs are installed between Nodes 55 and 95, and Nodes 117 and 123. The installation information of SOPs and parameters of FDN are same as those in the modified IEEE 33-node test case.

The same Scenarios I and II in Section V.C are also carried out in the large-scale case. Tables IX and X list the operation performance of the two scenarios. The computational time for the modified IEEE 123-node test case is 2520.20s which is acceptable for the day-ahead flexibility pricing.

TABLE IX

FLEXIBILITY COSTS OF SCENARIOS I AND II

Scenario	$C^{sub,P}$ (USD)	$C^{sub,Q}$ (USD)	$C^{FR,P}$ (USD)	$C^{FR,Q}$ (USD)	C^{V} (USD)	C^{Res} (USD)	Total (USD)
I	93.5228	19.7145	0.0000	-	81.0141	-	194.2514
II	91.5859	-8.6210	0.7467	12.7497	0.1081	15.4122	98.4852

TABLE X

FLEXIBILITY PERFORMANCE COMPARISON OF SCENARIOS I AND II

Scenario	Total loss (kWh)	Network loss (kWh)	Device loss (kWh)	Maximum loading rate (%)	Voltage (p.u.)	VDI
I	1426.8	1426.8	-	130.22	0.9096-1.0295	0.4441
II	1032.3	946.2	86.0	99.64	0.9786-1.0394	0.0003

As shown in Tables IX and X, voltage violation and branch congestion in Scenario I indicate that the entire system without proper guides will have an obvious flexibility imbalance. The voltage extreme in Scenario I is near the lower limit of allowable range although the total capacity of DGs is almost 100% of the test case. In Scenario II, flexible resources are coordinated under the guide of flexibility price. According to voltage deviation index, maximum loading rate and power losses, spatial-temporal balance of operational flexibility is improved. The total flexibility cost is reduced by 49.30% in Scenario II.

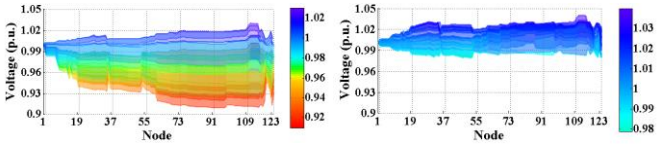

(a) Scenario I (b) Scenario II

Fig. 14 Voltage profiles of Scenarios I and II.

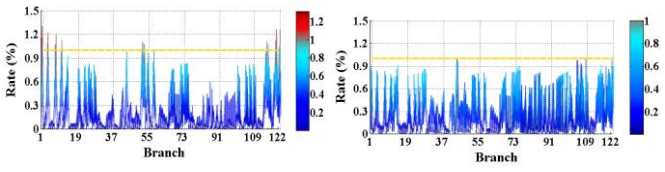

(a) Scenario I (b) Scenario II

Fig. 15 Branch loading ratios of Scenarios I and II.

Fig. 14 and Fig. 15 respectively illustrate the voltage profile of each node and loading ratio of each branch in a day of Scenarios I and II. The loading ratios of Branches 77-110 are increased as flexible resources at related nodes are guided to alleviate voltage deviation and branch congestion in other feeders. Hence, the system voltage profile is improved and branch congestion is avoided with a better balance of operational flexibility. In addition, the power purchased from

the upper grid is decreased, which shows better self-sufficiency under the proposed approach in Scenario II.

In summary, the DLMP-based flexibility price can be used to quantify the comprehensive impact on the node's supply or demand of operational flexibility service in the entire FDN. DSO can use the flexibility price to guide the flexible resources to achieve a better spatial-temporal balance of flexibility and effectively improve the comprehensive flexibility performance.

VI. Conclusions

This paper proposes a DLMP-based flexibility quantification and analysis method for FDNs. A generalized mathematical analytic framework is proposed for flexibility quantification and transfer analysis to achieve a feasible balance of diversified flexibility requirements in FDNs. Flexibility sensitivity factors are derived to analytically represent the spatial-temporal transfer relationship of operational flexibility. Then, a DLMP-based flexibility pricing method is proposed to quantify the flexibility value and determine the amount of nodal net active and reactive power. The spatial-temporal impacts of nodal net power on operational flexibility in FDNs are quantified in the form of price which can be used to dispatch flexible resources. Finally, the effectiveness is validated on a modified IEEE 33-node test case and a modified IEEE 123-node test case. Results show that the flexibility price can motivate multiple flexible resources to contribute to operating performance improvement. There is a feasible solution to achieve the comprehensive improvement in power loss reduction, voltage profile enhancement, branch congestion mitigation, and less dependence on power purchased from upper grid. The proposed method further provides an explicit analytic solution that can satisfy diversified flexibility requirements without violating various operational constraints in FDNs.

There are several directions to explore in our future work. First, the proposed analytic framework of operational flexibility will be extended to price the flexibility reserve to cope with DER uncertainties. Moreover, DLMP-based flexibility pricing can combine with game theory to motivate flexible resources to participate in peer-to-peer trading of flexibility services. Further, the DLMP-based flexibility analysis can be applied in the allocation of flexible resources to enhance operational flexibility of FDNs. Additionally, the coupling impact of active power and reactive power on flexibility is to be investigated in depth to improve the computation accuracy of flexibility price.

Appendix A

For the sake of analysis, nodes in the distribution network with radial topology are numbered from the source node. The node incidence matrix $\boldsymbol{A}^{N_\mathrm{n}\times N_\mathrm{n}}$ is defined as follows.

$$A(i,j)=\begin{cases}1, & \text{if node } j \text{ belongs to the sub-tree of node } i\\ 0, & \text{if node } j \text{ does not belong to the sub-tree of node } i\end{cases} \tag{A.a}$$

It is specified that branch l with node k as the downstream node is numbered as L_{k-1}. Node k and the nodes belonging to node k's sub-tree ($A(k,i)=1$) are the general downstream nodes of branch l. The general branch-node incidence matrix $\boldsymbol{M}^{N_\mathrm{b}\times N_\mathrm{n}}$ is defined as follows.

$$M_{l-i}=A(k,i),\ i\in\{1,2,\dots,N_\mathrm{n}\}$$
$$M_{l-i}=\begin{cases}1, & \text{if node } i \text{ is the general downstream node of branch } l\\ 0, & \text{if node } i \text{ is not the general downstream node of branch } l\end{cases} \tag{A.b}$$

Appendix B

Operation constraints of devices

(1) Source side

Operation constraints of DG are shown as follows.

$$\begin{gathered}P_{i,t}^{\mathrm{DG}}=P_{i,t}^{\mathrm{DG,ref}}\\ (P_{i,t}^{\mathrm{DG}})^2+(Q_{i,t}^{\mathrm{DG}})^2\le(S_i^{\mathrm{DG}})^2\\ Q_{i,t}^{\mathrm{DG}\prime}\ge Q_{i,t}^{\mathrm{DG}},Q_{i,t}^{\mathrm{DG}\prime}\ge -Q_{i,t}^{\mathrm{DG}}\end{gathered} \tag{B.a}$$

where $Q_{i,t}^{\mathrm{DG}\prime}$ indicates the absolute value of reactive power of DG at node i in time t.

(2) Network side

a) Operation constraints of SOP

$$P_{i,t}^{\mathrm{SOP}}+P_{j,t}^{\mathrm{SOP}}+P_{i,t}^{\mathrm{SOP,L}}+P_{j,t}^{\mathrm{SOP,L}}=0,\ \forall i,j\in\Omega_{\mathrm{SOP}} \tag{B.b}$$

$$\alpha_{c,0}P_{i,t}^{\mathrm{SOP}}+\alpha_{c,1}Q_{i,t}^{\mathrm{SOP}}+\alpha_{c,2}S_i^{\mathrm{SOP}}\le 0,\forall c\in\{1,2,\dots,12\} \tag{B.c}$$

$$\alpha_{c,0}P_{i,t}^{\mathrm{SOP}}+\alpha_{c,1}Q_{i,t}^{\mathrm{SOP}}+\alpha_{c,2}\frac{P_{i,t}^{\mathrm{SOP,L}}}{A_i^{\mathrm{S,L}}}\le 0,\forall c\in\{1,2,\dots,12\} \tag{B.d}$$

$$\underline{P}_i^{\mathrm{SOP}}\le P_{i,t}^{\mathrm{SOP}}\le\bar{P}_i^{\mathrm{SOP}},\underline{Q}_i^{\mathrm{SOP}}\le Q_{i,t}^{\mathrm{SOP}}\le\bar{Q}_i^{\mathrm{SOP}} \tag{B.e}$$

where (B.b) is the power balance constraint. (B.c) is the linearized SOP capacity constraint. (B.d) is the operational loss constraint after convex relaxation and linearization [8]. The non-linear capacity constraints and loss constraints of devices are linearized through the approximate polygon method.

b) Operation constraints of ESS

$$E_{i,t}^{\mathrm{ESS}}=E_{i,t-1}^{\mathrm{ESS}}-(P_{i,t}^{\mathrm{ESS}}+P_{i,t}^{\mathrm{ESS,L}})\Delta t,\ \forall i\in\Omega_{\mathrm{ESS}} \tag{B.f}$$

$$\underline{E}_i^{\mathrm{ESS}}\le E_{i,t}^{\mathrm{ESS}}\le\bar{E}_i^{\mathrm{ESS}} \tag{B.g}$$

$$E_{i,\mathrm{T}}^{\mathrm{ESS}}=E_{i,0}^{\mathrm{ESS}} \tag{B.h}$$

$$\underline{P}_i^{\mathrm{ESS}}\le P_{i,t}^{\mathrm{ESS}}\le\bar{P}_i^{\mathrm{ESS}},\underline{Q}_i^{\mathrm{ESS}}\le Q_{i,t}^{\mathrm{ESS}}\le\bar{Q}_i^{\mathrm{ESS}} \tag{B.i}$$

$$\alpha_{c,0}P_{i,t}^{\mathrm{ESS}}+\alpha_{c,1}Q_{i,t}^{\mathrm{ESS}}+\alpha_{c,2}S_i^{\mathrm{ESS}}\le 0,\forall c\in\{1,2,\dots,12\} \tag{B.j}$$

$$\alpha_{c,0}P_{i,t}^{\mathrm{ESS}}+\alpha_{c,1}Q_{i,t}^{\mathrm{ESS}}+\alpha_{c,2}\frac{P_{i,t}^{\mathrm{ESS,L}}}{A_i^{\mathrm{E,L}}}\le 0,\forall c\in\{1,2,\dots,12\} \tag{B.k}$$

where (B.f)-(B.h) are the SOC constraints. (B.j) and (B.k) are the linearized capacity constraint and loss constraint, respectively.

(3) Demand side

a) Operation constraints of DL

The power consumption of DL can respond to TOU and flexibility requirements as long as the charging demand can be satisfied within its available time. Electric vehicles and data centers are typical of DLs.

$$\begin{gathered}0\le P_{i,t}^{\mathrm{DL}}\le\bar{P}_i^{\mathrm{DL}}\\ 0\le Q_{i,t}^{\mathrm{DL}}\le P_{i,t}^{\mathrm{DL}}\cdot\tan(\cos^{-1}\vartheta_i^{\mathrm{DL}})\\ E_{i,t}^{\mathrm{DL}}\ge E_i^{\mathrm{DL,req}},t\ge T_{i,\mathrm{req}}^{\mathrm{DL}}\\ E_{i,t}^{\mathrm{DL}}=E_{i,t-1}^{\mathrm{DL}}+P_{i,t}^{\mathrm{DL}}\Delta t,\ \mathrm{T}_{i,\mathrm{start}}^{\mathrm{DL}}\le t\le T_{i,\mathrm{req}}^{\mathrm{DL}}\end{gathered} \tag{B.l}$$

where $\vartheta_i^{\mathrm{DL}}$ is the power factor of DL at node i.

b) Operation constraints of TL

The power consumption of TL must be satisfied at once based on the pre-determined schedule.

$$P_{i,t}^{\mathrm{TL}}=P_{i,t}^{\mathrm{TL,ref}},Q_{i,t}^{\mathrm{TL}}=Q_{i,t}^{\mathrm{TL,ref}} \tag{B.m}$$

REFERENCES

[1] International Renewable Energy Agency. (2019) Renewable energy statistics 2019. [Online]. Available: https://www.irena.org/publications/2019/Jul/Renewable-energy-statistics-2019.

[2] S. Riaz and P. Mancarella, "Modelling and characterisation of flexibility from distributed energy resources," *IEEE Trans. Power Syst.*, vol. 37, no. 1, pp. 38-50, 2022.

[3] L. Fang, K. Ma, F. Li, *et al*, "A new incentive scheme to incentivize flexible customers for phase balancing," *CSEE J. Power Energy Syst.*, 2022, Early Access.

[4] B. Park, Y. Chen, M. Olama, *et al*, "Optimal demand response incorporating distribution LMP with PV generation uncertainty," *IEEE Trans. Power Syst.*, vol. 37, no. 2, pp. 982-995, 2022.

[5] J. Xiao, Y. Wang, F. Luo, *et al*, "Flexible distribution network: definition, configuration, operation, and pilot project," *IET Gener. Transm. Distrib.*, vol. 12, no. 20, pp. 4492-4498, 2018.

[6] M. Kalantar-Neyestanaki and R. Cherkaoui, "Coordinating distributed energy resources and utility-scale battery energy storage system for power flexibility provision under uncertainty," *IEEE Trans. Sustain. Energy*, vol. 12, no. 4, pp. 1853-1863, 2021.

[7] J. Ma, V. Silva, R. Belhomme, *et al*, "Evaluating and planning flexibility in sustainable power systems," *IEEE Trans. Sustain. Energy*, vol. 4, no. 1, pp. 200-209, 2013.

[8] H. Ji, C. Wang, P. Li, *et al*, "Quantified analysis method for operational flexibility of active distribution networks with high penetration of distributed generators," *Appl. Energy*, vol. 239, pp. 706-714, 2019.

[9] A. Ulbig and G. Andersson, "Analyzing operational flexibility of electric power systems," *Int. J. Electr. Power Energy Syst.*, vol. 72, pp. 155-164, 2015.

[10] North American Electric Reliability Corporation, "2020 State of reliability," USA: North American Electric Reliability Council; 2020.

[11] International Energy Agency, "The power of transformation: wind, sun and the economics of flexible power systems," Paris: International Energy Agency; 2014.

[12] E. Lannoye, D. Flynn, M. O'Malley, "Evaluation of power system flexibility," *IEEE Trans. Power Syst.*, vol. 27, no. 2, pp. 922-931, 2012.

[13] Z. Lu, H. Li, and Y. Qiao, "Probabilistic flexibility evaluation for power system planning considering its association with renewable power curtailment," *IEEE Trans. Power Syst*., vol. 33, no. 3, pp. 3285-3295, 2018.

[14] J. Zhao, T. Zheng, and E. Litvinov, "A unified framework for defining and measuring flexibility in power system," *IEEE Trans. Power Syst.*, vol. 31, no. 1, pp.339-347, 2016.

[15] W. Wei, Y. Chen, C. Wang, *et al*, "Nodal flexibility requirements for tackling renewable power fluctuations," *IEEE Trans. Power Syst.*, vol. 36, no. 4, pp. 3227-3237, 2021.

[16] X. Chen, E. Anese, C. Zhao, *et al*, "Aggregate power flexibility in unbalanced distribution systems," *IEEE Trans. Smart Grid*, vol. 11, no. 1, pp. 258-269, 2020.

[17] Y. Liu, Z. Li, W. Wei, J. H. Zheng and H. Zhang, "Data-driven dispatchable regions with potentially active boundaries for renewable power generation: Concept and construction," *IEEE Trans. Sustain. Energy*, vol. 13, no. 2, pp. 882-891, 2022.

[18] S. Wang and W. Wu, "Aggregate flexibility of virtual power plants with temporal coupling constraints," *IEEE Trans. Smart Grid*, vol. 12, no. 6, pp. 5043-5051, 2021.

[19] L. Fan, C. Zhao, G. Zhang, *et al*, "Flexibility management in economic dispatch with dynamic automatic generation control," *IEEE Trans. Power Syst.*, vol. 37, no. 2, 2021.

[20] S. Torbaghan, G. Suryanarayana, H. Höschle, *et al*, "Optimal flexibility dispatch problem using second-order cone relaxation of ac power flows," *IEEE Trans. Power Syst.*, vol. 35, no. 1, pp. 98-108, 2020.

[21] X. Yang, C. Xu, H. He, *et al*, "Flexibility provisions in active distribution networks with uncertainties," *IEEE Trans. Sustain. Energy*, vol. 12, no. 1, pp. 553-567, 2021.

[22] M. R. M. Cruz, D. Z. Fitiwi, S. F. Santos, *et al*, "Multi-flexibility option integration to cope with large-scale integration of renewables," *IEEE Trans. Sustain. Energy*, vol. 11, no. 1, pp. 48-60, 2020.

[23] X. Yan, C. Gu, H. Zhang, *et al*, "Network pricing with investment waiting cost based on real options under uncertainties," *IEEE Trans. Power Syst.*, 2022, Early Access.

[24] H. Chen, L. Fu, L. Bai, *et al*, "Distribution market-clearing and pricing considering coordination of DSOs and ISO: an EPEC approach," *IEEE Trans. Smart Grid*, vol. 12, no. 4, pp. 3150-3162, 2021.

[25] X. Yan, C. Gu, F. Li, *et al*, "LMP-based pricing for energy storage in local market to facilitate PV penetration," *IEEE Trans. Power Syst.*, vol. 33, no. 3, pp. 3373-3382, 2018.

[26] J. Wei, Y. Zhang, J. Wang, *et al*, "Distribution LMP-based demand management in industrial park via a bi-level programming approach," *IEEE Trans. Sustain. Energy*, vol. 12, no. 3, pp. 1695-1706, 2021.

[27] Q. Hu, F. Li, X. Fang and L. Bai, "A framework of residential demand aggregation with financial incentives," *IEEE Trans. Smart Grid*, vol. 9, no. 1, pp. 497-505, 2018.

[28] Z. Liu, Q. Wu, S. Oren, *et al*, "Distribution Locational Marginal Pricing for Optimal Electric Vehicle Charging Through Chance Constrained Mixed-Integer Programming," *IEEE Trans. Smart Grid*, vol. 9, no. 2, pp. 644-654, 2018.

[29] F. Meng, B. H. Chowdhury, and M. Chamana, "Three-phase optimal power flow for market-based control and optimization of distributed generations," *IEEE Trans. Smart Grid*, vol. 9, no. 4, pp. 3691-3700, 2018.

[30] Z. Liu, Q. Wu, S. S. Oren, *et al*, "Distribution locational marginal pricing for optimal electric vehicle charging through chance constrained mixed-integer programming," *IEEE Trans. Smart Grid*, vol. 9, no.2, pp. 644-654, 2018.

[31] J. Wei, Y. Zhang, F. Sahriatzadeh, *et al*, "DLMP using three-phase current injection OPF with renewables and demand response," *IET Renew. Power Gener.*, vol. 13, no. 7, pp. 1160-1167, 2019.

[32] H. Yuan, F. Li, Y. Wei, *et al*, "Novel linearized power flow and linearized OPF models for active distribution networks with application in distribution LMP," *IEEE Trans. Smart Grid*, vol. 9, no. 1, pp. 438-448, 2018.

[33] K. Zhang, S. Troitzsch, S. Hanid, *et al*, "Coordinated market design for peer-to-peer energy trade and ancillary services in distribution grids," *IEEE Trans. Smart Grid*, vol. 11, no. 4, pp. 2929-2941, 2020.

[34] M. Faqiry, L. Wang, and H. Wu, "HEMS-enabled transactive flexibility in real-time operation of three-phase unbalanced distribution systems," *J. Mod. Power Sys. Clean Energy*, vol. 7, no. 6, pp. 1434-1449, 2019.

[35] S. Huang, Q. Wu, S. Oren, *et al*, "Distribution locational marginal pricing through quadratic programming for congestion management in distribution networks," *IEEE Trans. Power Syst.*, vol. 30, no. 4, pp. 2170-2178, 2015.

[36] F. Li and R. Bo, "DCOPF-based LMP simulation: algorithm, comparison with ACOPF, and sensitivity," *IEEE Trans. Power Syst.*, vol. 22, no. 4, pp. 1475-1485, 2007.

[37] L. Bai, J. Wang, C. Wang, *et al*, "Distribution locational marginal pricing (DLMP) for congestion management and voltage support," *IEEE Trans. Power Syst.*, vol. 33, no. 4, pp. 4061-4073, 2018.

[38] L. González-Sotres, P. Frías, and C. Mateo, "Techno-economic assessment of forecasting and communication on centralized voltage control with high PV penetration," *Electr. Power Syst. Res.*, vol. 151, pp. 338-3447, 2017.

[39] J. Bloemink, T. Green, "Benefits of distribution-level power electronics for supporting distributed generation growth," *IEEE Trans. Power Deliv.*, vol. 28, no. 2, pp. 911-919, 2013.

[40] Y. Liu, Z. Tang, and L. Wu, "On secured spinning reserve deployment of energy-limited resources against contingencies," *IEEE Trans. Power Syst*., vol. 37, no. 1, pp. 518-529, 2021.

[41] M. Farivar and S. H. Low, "Branch flow model: Relaxations and convexification-parts I," *IEEE Trans. Power Syst*., vol. 28, no. 3, pp. 2554-2564, 2013.

[42] J. Lofberg. "Yalmip: A toolbox for modeling and optimization in MATLAB," *in Proc. CASCD Conf*., pp. 284-289, 2004.

[43] K. Chen, W. Wu, and B. Zhang, "Robust restoration method for active distribution networks," *IEEE Trans. Power Syst.*, vol. 31, no. 5, pp. 4005-4015, 2016.